CHALMERS

Advanced signal processing techniques for pulsed-doppler radar

Master of Science Thesis

KARIM OUNISSI

Department of Signals and Systems
Division of Signal Processing and Antennas
CHALMERS UNIVERSITY OF TECHNOLOGY
Göteborg, Sweden, 2006
Report No. EX083/2006

Advanced Signal Processing Techniques For Pulsed-Doppler Radar

Karim Ounissi

November 27, 2006

Advanced Signal Processing Techniques For Pulsed-Doppler Radar

Karim OUNISSI

This document has been written using LaTeX

Technical Report No. EX083/2006
School of Electrical Engineering
Chalmers University of Technology Signal Processing Group

Department of Signals and Systems
Chalmers University of Technology
SE-412 96 Göteborg, Sweden
Telephone : +46(0)31-772 1000

Abstract

This Master Thesis deals with Radar Signal Processing techniques. The scope of the thesis is to present state-of-the-art digital signal processing techniques for Pulsed-Doppler radar. This includes target detection and velocity estimation in a battle field. The reader will be given a short introduction on Radar fundamentals and then a block-based analysis will follow. Lastly, figures will depict an example scenario.
Part one gives an overall overview of how a Radar is composed in terms of system elements. We will see that a radar system design strongly depends on what the radar mission is, i.e. target detection, target ranging, target tracking. From this important choice, system's components and signal processing techniques are selected from a wide range of available techniques.
Part two describes and details radar signal processing flow. Provided numbers and examples show how powerfull a military radar system is regarding to its difficult mission. Pulsed-Doppler radars are capable of ranging a target while also estimating its relative radial speed. Accurate ranging strongly relies on the Pulse Compression technique, whereas Doppler filtering allows velocity estimation. ACP and CFAR blocks tend to first, combat environment noises such as sea and ground clutter, and second, to maintain radar performances by reducing false alarms.
Part three ends the thesis with figures showing the output of each studied block. The reader will see how noisy the received echo (backscaterred signal) is and how signal processing techniques can however recover information on the targets. Figures are taken from a Matlab© simulator developped in order to easily test new algorithms.

Keywords : *Radar, Digital Signal Processing, Antenna, Pulse-Compression, Ambiguity function, Doppler, Pulse-Doppler, Matched-Filter, MTI, CFAR, ACP, Noise, Clutter, RCS*

Table of Contents

List of Figures

Acknowledgements

This part of the Thesis is certainly the thoughest one to write. One does not know who to start with. So many people to thank, so many people to remember ... sorry for those of you I might forget but you know I still owe you everything. First of all, I would like to thank M. Meunier who gave me the chance to make my dream come true. I will never forget. God bless you.
Next, my thanks go to all the people I met during my studies from day one to today. They all taught me so much. From my teachers at my french school EFREI (Ecole FRançaise d'Electronique et d'Informatique) to my teachers at Chalmers University in Sweden, I really learnt a lot from all of you. I would like to express special thanks to Professor Erik Ström, Joakim Gunnarson, Professor Eric Agrell. My final year at Chalmers has been a wonderful time. A great life lesson and a rich cultural experience.
I would like to thank all the people from Thales Air Defence in Bagneux (France) who helped me to answer my [numerous] questions about radar techniques. Special thanks go to Geneviève Granier, Philippe Fauvet, Eric Billon, Frederico Garcia and Yves-André Caparro.
Last but not least, I would like to express my deep love to my family, from my Dad and my Mom to my two brothers and my little sister. Thank you all. You have been of a great help when things did not run well. You supported me and encouraged me to go for it. God bless you all.

Very special thanks to my Baby Love Oujdan

Abbrevations and Acronyms

ACP	Anti-Clutter Processor
AF	Ambiguity Function
AWGN	Additive White Gaussian Noise
CFAR	Constant False Alarm Rate
CW	Continuous Wave
DF	Doppler Filtering
DSP	Digital Signal Processing
ESEA	Electronically Steered Phased Antenna
FFT	Fast Fourier Transform
FIR	Finite Impulse Response
FM	Frequency Modulation
FT	Fourier Transform
IFF	Identification Friend or Foe
IFFT	Inverse Fast Fourier Transform
LT	Laplace Transform
MF	Matched Filter
MTD	Moving Target Detector
MTI	Moving Target Indicator
MPR	Mono-Pulse Radar
MRR	Multi-Role Radar
PC	Pulse Compression
PDF	Probability Density Function
PI	Post Integration
PT	Pulse Train
RADAR	RAdio Dection And Ranging
RCS	Radar Cross-Section
RF	Radio Frequency
SAR	Synthetic Aperture Radar
SMBAA	Simultaneous Multiple Beams Array Antenna
SPI	Slidding Post Integration
TWF	Time Weightning Function
WF	Whitening Filter

Introduction

The theme of the thesis is Advanced Signal Processing Techniques for Pulsed-Doppler Radar. As the title suggests, the paper deals with techniques, from a very low level point of view, that allow a radar to detect a target, estimate its parameters and track it in a noisy environment.
Nowadays, any military force has a set of various radars that perform several strategic and tactical missions. Radar systems are used in both civilian and military domains. Airports use radar systems to track landing aircrafts. Weather forecasts are mostly based on radar maps taken from satellites. Police forces use handed-Doppler radars to check car speed.
In the military domain, the missions of a radar range from target detection and target tracking (air defence) to counter-measures and battlefield surveillance. This thesis will only focus on target detection in noisy enviroments from a signal processing perspective. The main difference between the civilian and the military domains is the fact that in war context, targets try to escape from radar coverage whereas in civilian domain, the security of an aircraft is partly ensured by the radar coverage in case of dense air traffic. Moreover, in the civilian domain aircrafts do have similar shapes and volume; it strongly eases system design as all targets have similar caracteristics (mainly speed and shape). However, in the military domain, each side tries to have furtive vehicles that can get close to the opponent forces without being detected. This involves very complex architecture and structure designs. Each target has a so-called *radar signature*. Targets are classified according to specific (sometimes secret) criteria. Basically, it defines how a given target will respond to pre-defined specific electromagnetic signals. Materials used and body shape are of high importance in designing a furtive vehicle.
Radar Signal Processing involves mathematical function analysis and fundamental theory in several scientific fields (waves propagation, digital filtering...). A strong background in these areas is required in order to design such system. However, this paper will only explore the signal processing aspects of radar designing. It assumes that the reader has basic knowledge in electromagnetic wave theory, antenna theory and signal processing.

This document is based on the development of a radar signal processing simulator. The simulator is part of the contract that Thales Air Defence engineering teams in Bagneux (France) have signed for the delivery of a new military radar for Thales Naval Company. A simulator for the MRR - Multi-Role Radar - has been developped almost a decade ago using Matlab© software. The MRR-3D NG[1](3-Dimension New Generation) radar is the new version of the MRR radar. The new version of the radar utilizes state-of-the-art signal processing algorithms. A new Matlab© simulator has been developped through the porting of the previous simulator from Windows© station to Linux© station. The new simulator provides an easy-to-use GUI, more display capabilities for intermediate signals, NetCDF© programming and a multi-scan operation mode. This last feature allows the user to display

[1]http://www.thales-naval.nl/naval/activities/radar-sys/surveillance/products/mmr.htm

outputs of some recursive algoritms as they require multiple scans to provide consistant results.

The MRR-3D NG is a system capable of:

- automatic detection and tracking of air targets whether sea-skimming or diving and whatever the antenna rotation speed
- transmission of very accurate 3D measurements for the most dangerous targets, to the management system, in order to reduce the weapon system reaction time, thus optimising the ship's response to the most threatening air targets
- detection and automatic tracking of surface targets, using a specific reception channel in both mode

The MRR radar falls in the middle range, 3D-air and surface surveillance category. It is designed as a flexible (add-in features in option are available for the customer), modern and automatic radar. It is mainly designed for ships, frigates. It also owns an IFF[2] system with its secondary antenna that allows supersonic-targets identification. The IFF system is a must-have component for state-of-the-art military radar.

The thesis is structured in three parts :

- Part I : a short historical overview of radar system origins in the time and a block-based picture of the MRR radar gives the reader a good understanding of what a radar is composed of
- Part II : a deep look into signal processing theory gives the understanding of Pulse-Doppler radar operation
- Part III : an application example is depicted throughout a Matlab-based radar signal processing simulator that shows outputs from major blocks in the signal flow

[2] http://www.dean-boys.com/extras/iff/iffqa.html

Figure 1: MRR in action

Part I

Background

Chapter 1

Introduction to radar theory: from history to today

Unlike what it is often written in the litterature, radar systems did not come out from one man's brain (i.e. Sir Watson-Watt, an english scientist), eventhough his work did contribuate to the birth of radar systems. Indeed, today modern radars are mostly the result of a constant effort in the scientific world. These efforts tended to enhance a previous invention made by a german scientist. In 1904, Christian Hulfsmeyer presented his *telemobiloscope*, an equipment that detects iron-made objetcs using self-generated electromagnetic waves.
During the 20s and the 30s, great progress has been made in battle between european scientists and american scientists. French scientists Pierret and Gutton, and US scientists Taylor and Young experienced new systems that use metric waves. However, at this time, radars were using continuous transmission technique leading to difficult range measurements. In 1935, Sir Watson-Watt and his team built up a radar that utilized short pulses to allow accurate target range measurements. At this time, US scientists teamed up with British scientists to continue developping the new short pulse technique. At this time in Europe, French teams, throughout CSF company, had a few centimetric-wave radar systems working.
The word *RADAR*, short for RAdio Detection And Ranging) appeared a long time after in the US. It was a secret project code that US Marines launched at this time. Radar systems were designed to both detect a target and determine its range as the acronym explicitely suggests.
More on radar systems history can be found in [Car87].

First, radars were developped for a military use but nowadays radar systems are widely used in the civilian area. It exists a wide range of various applications for radars. It is obvious that a unique radar system design would not fulfill every needs. Within the military domain itself, various radar systems exist depending on what mission the radar is expected to perform. Therefore, when designing a radar system, the first question that should be answered is *What missions do I want my radar to complete ?*

- detect a target: i.e. provide a basic boolean indicator stating if there is a target in the direction pointed by the antenna; a dual-antenna (Tx/Rx) CW (Continuous Wave) radar system can perform such basic target detection

- localize a target: i.e. determine its coordinates in the 3-dimensional space; in this case, a pulsed radar appears to perform the best compared to a CW radar system. In this case, one has also to choose between a mono-pulse radar (MPR) and a train-pulsed radar system. Such a choice may be based on the maximum range the radar is expected to reach, the 3D area it has to cover but also on other specific aspects [Tho82]

- evaluate target's relative speed: i.e. measuring the *radial* component of the target velocity vector relative to the transmitting antenna own speed (if the radar is mobile); direct measurement can be performed either by evaluating the so-called Dopple-Fizau [1] shift of a pure tone signal or by interpolating relative positions between consecutive pulses (this is called indirect measurement). As long as target coordinates are not of importance, a CW radar can perform speed estimation by simply transmitting two pure tone signals and computing the difference beat

- track a target: chasing a target requires to continuously evaluate the target position and relative speed

Moreover, there exists some others questions that need to be considered before starting any system design:

- radar is static or mobile? answer to this question has a direct impact on the power management and on the mechanical aspects of the radar

- environment is mainly ground or water or mixed? answer to this question has a direct impact on the embedded signal processing techniques as each type of noise - natural or not - requires specific processing. In the military domain, opponent counter-mesaure (jamming) has to be taken into account.

The first question is of main importance if we consider the radar from a overall system perspective. Indeed, new parameters affect target position and speed estimation whether the radar is static (ground equipment) or mobile (airborne embedded systems, ship/frigate embedded systems). All measurements are thus relative to the radar own position in the 3D space and to its own speed. Embedded radars encounter fast changing operation conditions as ship/fregate or aircraft are not strictly stable. The second question also strongly affects signal processing techniques as ground and water does not have the same impact and effects on electromagnetic waves. Environment is not a deterministic parameter; thus, it is necessary to best estimate it using statistical models. Different models apply for each type of clutter.
Nowadays, military radars generally work tight with weapons systems. Indeed, the radar is responsible to find out if threatening targets are able to attack and hit. It gives indicators and signals on detected targets to the weapon systems. Automatic response or human-guided decisions follow. Military radar can have very wide range coverage, i.e. almost 800-900 km. Civilian aircrafts can be detected by radars and considered as targets. In fact, each radar uses a secondary antenna to run the IFF protocol. Each civilian aircraft has a embedded transponder that broadcast a specific code recognized by every military forces to be a *friend* ID. More on primary and secondary systems in [Col85].

[1] Often simply called Doppler shift

Chapter 2

System architecure

A general picture of a radar system is depicted in figure 2.1. It is designed as block-based system. Each block has a specific operation. For instance, the duplexor switches back and forth from transmitting to receiving operation since a dual Tx/Rx antenna is used, the IF block shifts the high-frequency received signal to a lower intermediate frequency (IF).

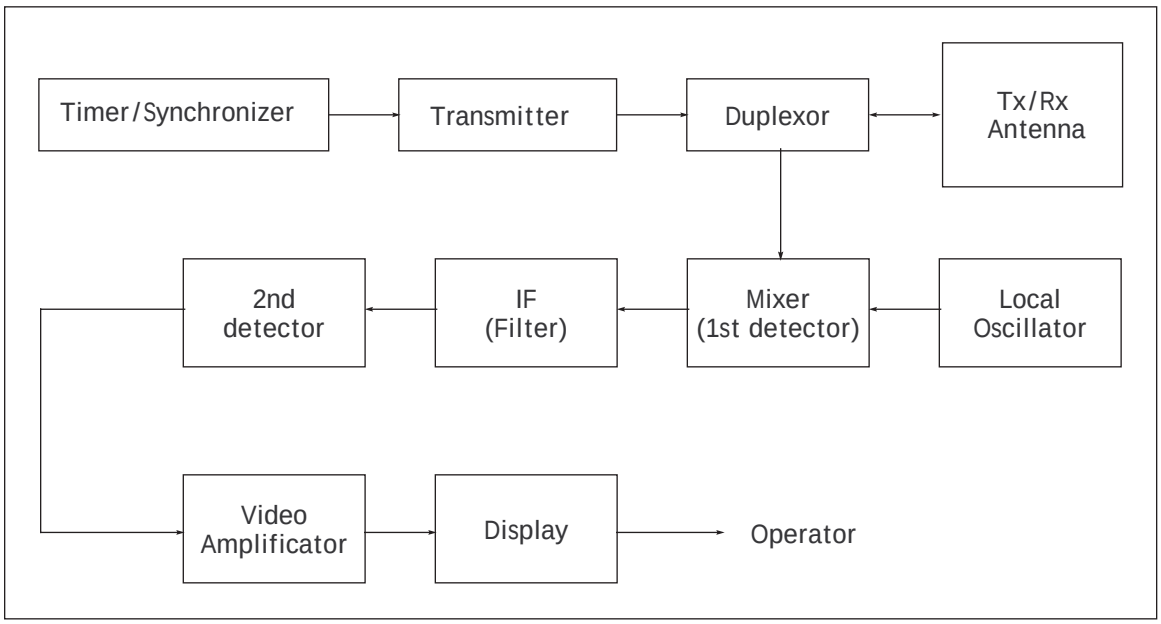

Figure 2.1: Radar General Model

The overall operation of the radar may look simple but it involves very fast and complex

mechanisms. Figure 2.2 details the core system of the MRR radar. It consists of several modules that interact one with each other in order to maximize automatic operation. Nowadays, human role is very limited in radar systems. The person in charge of operating the radar mainly decides on a limited range of options that sets the radar performance up. Most of the radar operation is automatic.

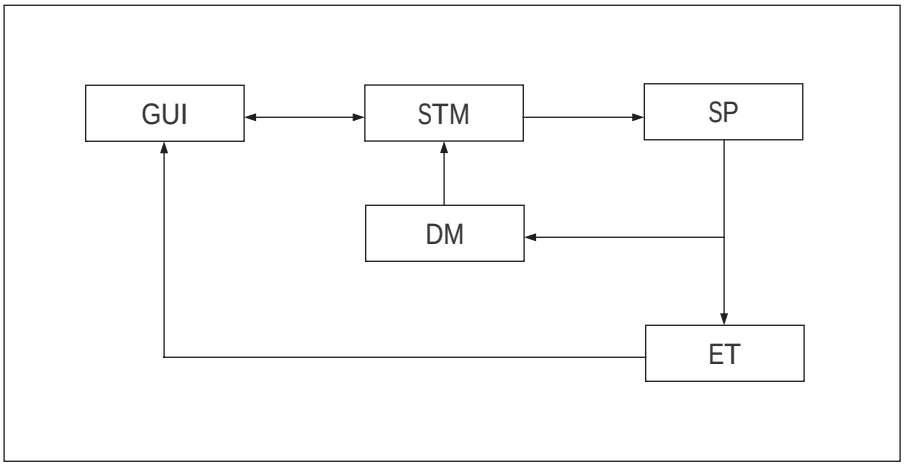

Figure 2.2: Radar synoptique

- GUI (Graphical User Interface): computer-based user interface including basic keyboard and mouse
- STM (Space-Time Management): system that monitors and controls the radar main functionalities such as space revolving, antenna pointing, waveform selection
- DM (Data Management): system that generates dynamic commands to the STM according to the ouputs from the SP block
- SP (Signal Processing): module that executes basic signal processing algorithms
- ET (Extract and Track): modules that extracts usefull information from the SP block output and performs target tracking

Basically, according to the situation, the radar can work in different *modes* that the operator selects via the GUI.

- altitude: scanning different slice of the 3D coverage volume (surface, low altitude, average altitude, high, altitude or very high altitude)
- filtering: Doppler targets or helicopters[1]
- tracking: multiple targets tracking enabled/disabled

[1]For helicopters, Doppler filtering requires specific filters due to the fast moving blades that generate a known Doppler flash

Part II

Study of RADAR Digital Signal Processing Techniques

Chapter 3

Signal Processing Techniques

3.1 Objectives et Problem definition

State-of-the-art digital circuits allow very fast computation and strong memory capacity for target ranging and detection. However, there exists a drawback in using digital computation rather than analogical signal processing. The radar coverage area has to be defined as a *discontinuous* area. The 3D area covered by the radar is seperated out in 2D maps. Each map is cut out in cells. This is mainly due to the fact that it strongly eases computation. Indeed, most of the signal processing is based on signal filtering. Moreover, in the distance/ranging domain the sampling frequency f_s defines the distance quantum[1] as $d_{min} = c/f_s$ where c is the light velocity. This gives the maximal accuracy of the radar on the range/distance dimension. In the azimuthal plane (horizontal/rotation plane), the 360° region is cut out in angle sectors. A value of about a hundred of angle sectors is expected for accurate coverage. Angle sectors are sometimes set to be equal to the 3dB beamwidth of the antenna eventhough this is not necessary. In the site plane (approximatively a 90°-wide angle), the altitude modes determine how many 2D area maps are to be stored. Basically, the radar operates in four or five distinct modes according to the altitude pointed by the antenna (the $3dB$ beamwidth also applies in the vertical plane). Moreover, the MRR is equipped with a SMBAA that allows to detect or track different target in the 3D space at the same time using multiple electronically-generated steered beams. For instance, the radar is capable of detecting an incoming opponent frigate (surface target) and at the same time, capable of tracking a helicopter (medium altitude).

3.2 Signal flow

Figure 3.1 shows the block-based structure of the signal processing techniques involved in the MRR radar. Each block has it own role in the target detection and/or tracking process. Shortly, we have:

- PC (Pulse Compression): it allows via specific filtering techniques to recover the transmitted signal from the noisy backscattered echo

[1] Quantum is the minimum distance unit

- AT (Amplitude Treatment): it gets rid of spurious values by checking every sample amplitude
- DF (Doppler Filtering): it evaluates the targets radial velocity through a bank of narrow-band filters
- ML (Module and Logarithm): it mathematically modifies the received signal in order to improve radar's detection capability
- ACP (Anti-Clutter Processor): it evaluates surrounding noise power according to the situation (sea, ground)
- CFAR (Constant False Alarm Rate): it adjusts detection thresholds and radar parameters in order to maintain detection performances
- PI (Post Integration): it combines pulses within a transmitted burst to improve target detection
- SPI (Sliding PI): it performs as PI but uses the output of PI from round to round
- Detection: it provides an indicator stating the presence of a target in each defined cell

The MRR 3D-NG has an optional feature called SLS, short for Side-Lobes-Suppression. Antenna theory shows that for any antenna design, the main lobe comes with small and often undesirable sidelobes that may degrade the received signal. The SLS algorithm tends to mathematically cancel out sidelobes drawbacks. Main lobe signal is composed of the desired echo signal with added noise such as jamming signals or clutter signals. Sidelobe signal mainly contains noise components. At the receiver stage, both sidelobes and mainlobe signals are mixed together. The use of an auxiliary antenna provides a way to theoretically suppress sidelobes signal. Signals received by the secondary antenna are scaled by an adaptive factor and substracted to the main antenna signal. The scaling factor is computed such that only the echo signal remains out of the received signal. Sidelobes effects are in practice strongly lowered.

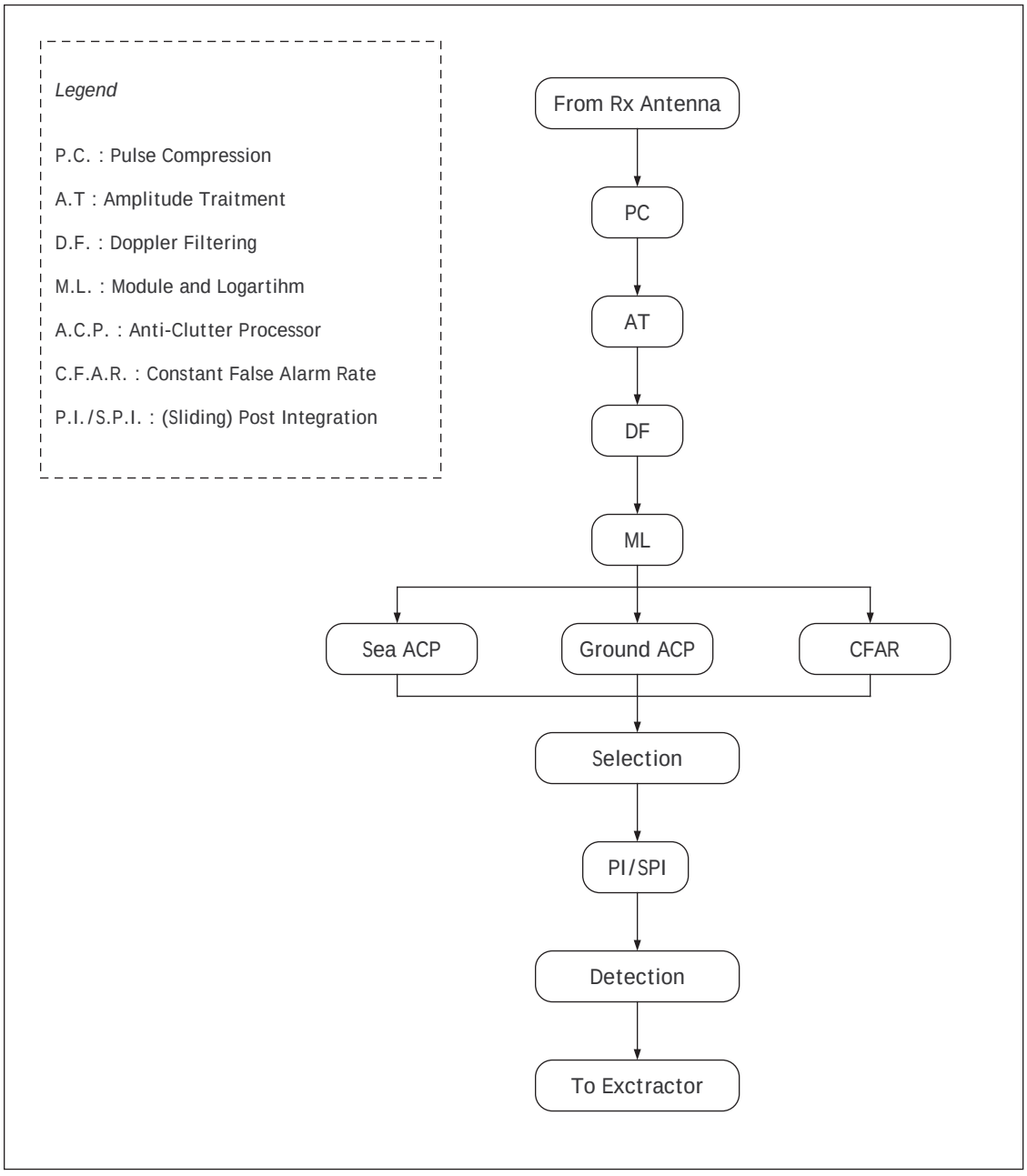

Figure 3.1: Signal Processing Signal Flow

Chapter 4

Basic Radar signal processing

4.1 Fundamentals

The use of electromagnetic waves in radar systems imposes some constraints on the overall performances. The basic concept of radars is to detect a target located at a distance denoted R by sending an electromagnetic wave through an antenna and measuring the time elapsed between the transmitted pulse and its received echo. According to optic/electromagnetic fundamental rules, this time denoted t_0 is directly proportional to the light velocity c:

$$t_0 = \frac{2R}{c}. \tag{4.1}$$

Equation (4.1) only gives information on the target range. Antenna theory states that the 3 dB beamwidth of an antenna is related to the carrier wavelength λ and the size of the antenna D in the given plane:

$$\theta_{3dB} \cong 70\frac{\lambda}{D}. \tag{4.2}$$

The direction of the target is directly given by the antenna pointing direction. Note that the accuracy of the direction estimation is increased by augmenting the antenna dimensions. Obviously, this leads to an unavoidable dilemma as radar system designs must meet practical constraints. For instance, embedded radar must have very limited dimensions. Thus, accuracy in the pointed direction is directly inverse proportional to the antenna dimensions (in a given plane).
With a pulsed radar, the signal to be transmitted is composed with a train of individual pulses, each pulse is shifted in time by T_R seconds. The pulse repetition frequency F_R is defined as:

$$F_R = \frac{1}{T_R}.$$

This parameter is involved in the calculation of the radar average transmitted power P_a:

$$P_a = P_p\frac{\tau}{T_R}, \tag{4.3}$$

where τ is the pulse duration, P_p is the peak power. The duty cycle, defined as $\frac{\tau}{T_R}$, provides information on radar average operation, one thousand is a common value.

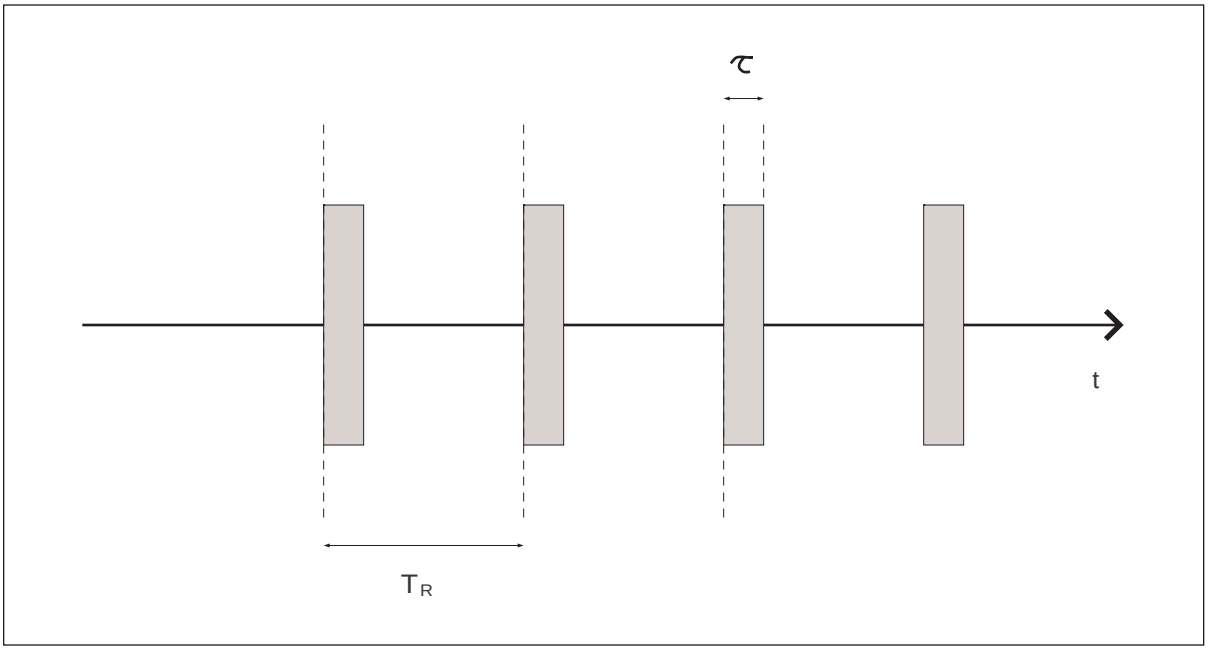

Figure 4.1: Pulses Burst diagram

For a pulsed radar, a new notion that does not exist in continuous-wave radar is defined: the range-discrimination factor. It is used in situations when two distinct targets are located in the same direction but at different ranges ($R_1 \neq R_2$). This means that both targets are located inside the antenna main-lobe. Thus, if the two targets respond to the transmitted signal by producing an echo, these echos are shifted in time such that:

$$\Delta t = \frac{2R_1}{c} - \frac{2R_2}{c} = \frac{2}{c}\Delta R \tag{4.4}$$

Each pulse has a duration equal to τ and if $\Delta t < \tau$, then the two echos overlap in time. If we only consider signal amplitude, the two signals may cancel each other in some points in time. One target may be hidden in such situation, that is not acceptable in a military context. The range-discrimination factor is defined as:

$$\Delta R = \frac{c\tau}{2} \tag{4.5}$$

Using the same concept, an angular-discrimation factor is defined. This radar parameter applies to both vertical (site) and horizontal (azimuthal) directions. It is defined in [Tho82] and expressed as follow:

$$\Delta\theta = 1.2\frac{\lambda}{D}. \tag{4.6}$$

4.2 Detection and Doppler effect

Recovering usefull information such as target position and relative velocity from the received signal strongly rely on stochastic processes estimation. The received signal is affected by two factors: random noise and unknown delay. Recovering information from a noisy signal can be roughly summarized as a detection probability function of the signal to noise ratio (SNR).
If we defined $\rho = s/N_0$ as the SNR where s is the minimal signal that the radar can exploit and N_0 is the noise density expressed in $[W/Hz]$, thus the maximal range R_{max} in meter that the radar is able to detect can be derived as follow.
Let us define the power density of an isotropic antenna, denoted P_{ia} at a distance R:

$$P_{ia} = \frac{P_t}{4\pi R^2}. \tag{4.7}$$

Radars employ directive antenna with gain G in the pointed direction. The power density for a directive antenna is written as:

$$P_{da} = P_{ia} \times G = \frac{P_t G}{4\pi R^2}. \tag{4.8}$$

Target echo signals reradiate back only a certain amount of the transmitted power, this amount is denoted σ and is called the radar cross section. It has units of area. The power density of a received echo signal is expressed as:

$$\begin{aligned} P_e &= \frac{P_t G}{4\pi R^2} \times \frac{\sigma}{4\pi R^2} \\ &= \frac{P_t G \sigma}{(4\pi^2)\, R^4}. \end{aligned} \tag{4.9}$$

The received power is only a fractional part of the transmitted power. This is due to the fact that antennas present an efficiency, denoted A_e that is less than unity (common values for the antenna aperture are in the range $0.7 - 0.85$). The maximal radar range R_{max} is the distance beyond which the target cannot be detected. This distance occurs when the received echo signal equals the minimum detectable signal S_{min}.

$$R_{max} = \left[\frac{P_t G A_e \sigma}{(4\pi)^2 S_{min}} \right]^{\frac{1}{4}}. \tag{4.10}$$

Equation (4.10) is called the *radar equation*. More on the radar equation and its various form and derivations in [Sko80].

Radar Cross Section (RCS) is a target parameter that allows to define how furtive the target is. It charaterizes how much of the transmitted signal is backscattered by the target. It is defined in $[m^2]$ and is often referenced as the virtual area of a target.

$$\sigma_{RCS} = 4\pi R^2 \frac{|E_r|^2}{|E_i|^2}, \tag{4.11}$$

where

- R: target range in $[m]$

- E_r: reflected electrical field in $[V/m^2]$
- E_i: in-coming electrical field in $[V/m^2]$

It appears that the RCS value of the target can be viewed as a random variable. Indeed, it changes over time and over space. At a given instant, the target presents a certain angle with respect to the vectors $\vec{E_i}$ and $\vec{E_r}$. The fact that the target is moving obviously modifies those angles and thus the leading value of σ_{RCS}. Some common average values are listed in table 4.1:

Target	*RCS* $[m^2]$
furtive target	0.01
UAV (Unmanned Aircraft Vehicle)	0.1
fighter aircraft	1
intercontinental aircraft	100

Table 4.1: Radar Cross Section examples

The minimum detectable signal S_{min} can be expressed in terms of minimum signal to noise ratio:

$$S_{min} = kT_0B_nF_n\left(\frac{S_0}{N_0}\right)_{min}, \tag{4.12}$$

where

- k: Boltzman constant in $[J/K]$
- T_0: system equivalent temperature in $[K]$
- B_n: receiver 3dB-bandwidth in $[Hz]$
- F_n: system noise figure $[/]$
- N_0: noise output from receiver $[W]$
- S_0: input signal power $[W]$

We can rewrite equation (4.10) including spare losses (L_i) due to system losses (plumbing loss due to RF transmission lines and connectors imperfection, beam-shape loss due to non-constant gain in the main lobe). More on specific radar system losses in [Sko80].

$$R^4_{max} = \frac{P_tGA_e\sigma}{(4\pi)^2kT_0B_nF_n\left(\frac{S_0}{N_0}\right)_{min}\sum_{i=0}^{+\infty}L_i}. \tag{4.13}$$

The receiver bandwidth must be carefully chosen since it directly impacts on the system perfomance. A large bandwidth causes noise to be added to the received signal and a too small value may cause useful signal to be filtered out. Recall that in our case (pulsed radar), the duration of a pulse is set equal to τ. It is easy to think that if we set the bandwidth B_n to be chosen as $B_n = 1/\tau$, we should have the optimum value if we consider that the energy

of the pulse is concentrated in the main lobe. Some experimental studies at the Boston MIT Radiation Laboratory[1] showed that the optimum value has to be chosen such that:

$$B_n = \frac{1.2}{\tau}. \tag{4.14}$$

An empirical formula, named Haeff formula ([Tho82]) gives the degradation coefficient by which the signal-to-noise ratio is multiplied if the receiver bandwidth is not chosen as $B_n = \frac{1.2}{\tau}$.

$$C = \frac{B\tau}{4\alpha}\left(1 + \frac{\alpha}{B\tau}\right)^2 [dB], \tag{4.15}$$

where

- B: bandwidth $[Mhz]$
- τ: pulse duration $[\mu s]$
- α: $\frac{B}{B_0}$ if we set[2] $B_0 = \frac{1}{\tau}$

If we use a value of B_n different from the optimum, the signal to noise ratio gets degraded ([Tho82, p. 26]). Thus, if we want to maintain a certain operational quality, say the probability of detection, we must increase the signal-to-noise ratio defined in (4.13). In case of a CW radar, equation (4.14) obviously does not apply since there is no signal duration τ.
The Pulsed-Doppler radar is capable of evaluating the target *relative* speed using the properties of the Doppler effect. The main property of the Doppler effect is that it produces a frequency shift which value is directly proportional to the target speed. However, frequency shift is only proportional to the *radial* component of the relative speed vector. Speed vector tangential component does not contribuate to the frequency shift. This is of very high importance because in some situations, the target may have a non-zero speed but does not produce Doppler effect as it is moving in circles around the radar position. Thus, it becomes impossible to estimate target speed by Doppler filtering means in such situation. Hopefully, another method exists to determine a target speed. It is possible as said before to extrapolate successive detected positions. Hence, it becomes easy to completely determine target velocity characteristics and path.
Doppler shift, denoted f_d, is given by the following expression where v_r stands for target radial relative velocity in $[m/s]$:

$$f_d = \frac{2v_r}{\lambda_0} = \frac{2v_r f_0}{c} \tag{4.16}$$

where

- λ_0: carrier wave length $[m]$
- f_0: carrier frequency $[Hz]$
- c: light velocity $[m/s]$

[1] It is possible to approximatively demonstrate $B_n = 1/\tau$, [Car62, chap. 12]
[2] α is only defined if B_0 is considered to be equal to $\frac{1}{\tau}$

4.3 Measurements accuracy

The position of the target is given by computing a time instant t_0 in the received signal $y(t)$ such that:

$$\begin{aligned} t_0 &= \arg\max_{t\in R^+} y(t) \\ &= \arg\max_{t\in R^+} \{(x(t)+n(t)) * h(t)\}, \end{aligned} \tag{4.17}$$

where $x(t)$ is the transmitted signal and $n(t)$ is an additive white complex noise (not necesseraly Gaussian) and $h(t)$ is the receiver filter. In case of a noise free environment, i.e. $n(t) = 0$, the time instant basically equals to zero. However, in a noisy environment, it has been shown that t_0 is a Gaussian random variable with mean and standard deviation such that:

$$\mu_{t_0} = 0, \tag{4.18}$$

$$\sigma_{t_0} = \frac{1}{2\pi\beta_0\sqrt{\frac{S_0}{N_0}}}, \tag{4.19}$$

with

$$\beta_0^2 = \frac{\int_{-\infty}^{+\infty} f^2 \left|H(f)\right|^2 df}{\int_{-\infty}^{+\infty} \left|H(f)\right|^2 df}, \tag{4.20}$$

where $H(f)$ is the Fourier transform of $h(t)$. These formulas, known as the Woodard formulas, lead to an error in range estimation such that

$$\sigma_R = \frac{c}{4\pi\beta_0\sqrt{\frac{S_0}{N_0}}}. \tag{4.21}$$

In the same way, it has been shown that the accuracy in Doppler-shift measurement is also linked to the ratio $\frac{S_0}{N_0}$.

$$\sigma_{f_d} = \frac{1}{2\pi T_f\sqrt{\frac{S_0}{N_0}}}, \tag{4.22}$$

$$\sigma_{v_r} = \frac{\lambda}{4\pi T_f\sqrt{\frac{S_0}{N_0}}}, \tag{4.23}$$

$$T_f^2 = \frac{\int_{-\infty}^{+\infty} t^2 \left|h(t)\right|^2 dt}{\int_{-\infty}^{+\infty} \left|h(t)\right|^2 dt}. \tag{4.24}$$

Parameters β_0^2 and T_f^2 are respectively called the second central moment of $|H(f)|^2$ and $|h(t)|^2$.
These equations can be used as a help to accurately determine the target position and radial velocity. They demonstrate the importante role of the signal-to-noise ratio in the overall performance. It shows that signal processing techniques involved tend to maximize signal-to-noise ratio in order to improve performance.

Chapter 5

Pulse Compression

5.1 Objective

The pulse compression block is the first stage of the signal processing chain. At the input of the module, the received signal is very noisy and almost looks like white noise (random values spread over all frequencies, see figure 10.2). The pulse compression technique tries to make the transmitted signal visible and dominant over the background noise. Unlike the pulses depicted in figure 4.1, the transmitted signal does not consist of basic rectangular-like pulses with constant amplitude and duration τ. The main reason is due to electromagnetic laws that do not permit low-frequencies signal to be sent over the air. Therefore there is a need to shift the signal on a carrier signal (a pure tone with high frequency[1]). Moreover, the system generates internal noise. The noise power decays in $1/f$. Thus, system self-generated noise is inversely proportional to the frequency. This gives a second good reason to use a carrier signal to transmit the signal. A basic quadratic demodulator recovers the signal from the RF modulation. The detected signal is shifted back to the baseband domain. Using a specific receiving filter, the output produces a triangular-like signal which maximum value leads to the target range.

5.2 Principle

Pulse Compression is involved in radar systems where both maximum detection range and range discriminator factor are of importance. Recall that combining equation (4.3) and (4.13), it is obvious that the maximum detection range R_{max} is proportional to the pulse duration τ. On the other hand, recall that the range discriminator factor d is $d = \frac{c\tau}{2}$ and this parameter must be minimized to ensure multiple targets detection. Obviously, it appears that it is impossible to have optimum values for both parameters. One first idea could be to increase the peak power while keeping the pulse duration to a low value, thus increasing the maximum range detection. However, due to hardware constraints, this solution is not feasable. The most popular solution consists in the use of particular pulses, called compressed pulses.

[1] in the GHz domain

Compressed pulses are pulses that have the particularity to have a non-zero duration[2] T at transmitting point such that $T >> \tau$. At the receiving point, their duration is set back to τ after filtering. We define

$$\rho = T/\tau \tag{5.1}$$

as the compression rate. Basic rectangular pulses on a carrier do not allow such results. It is necessary to add a modulation or coding scheme on the signal phase. The most popular coding scheme is the so-called *chirp* scheme.

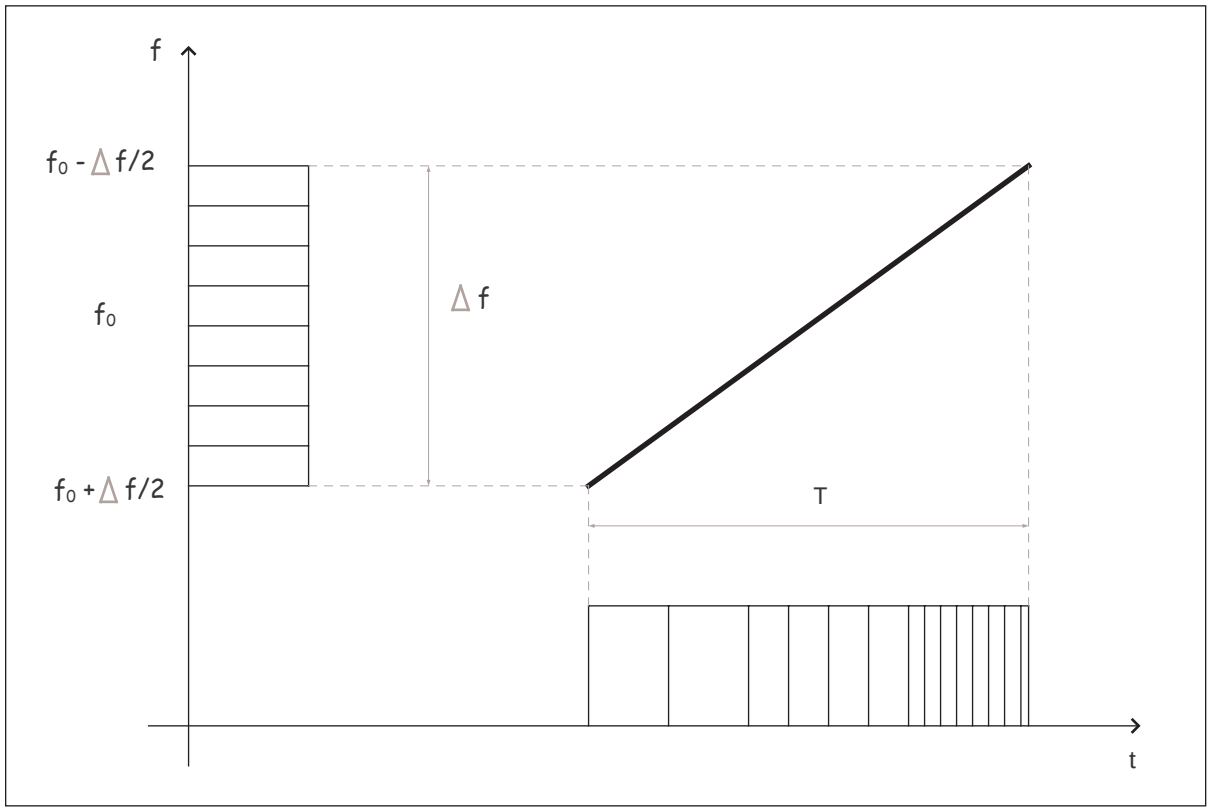

Figure 5.1: Pulse Compression principle

Figure 5.1 depicts the basic principle of the pulse compression. The frequency of a signal (a pure tone) is linearly modulated in the frequency range $[f_0 - \Delta f/2, f_0 + \Delta f/2]$ over the pulse duration T where f_0 is the carrier frequency. Thus, the transmitted signal is a repetition of frequency modulated pulses of duration T.

[2]Do not confuse T and T_R : T represents the duration during which power is transmitted whereas T_R denotes the whole pulse duration (see figure 4.1

5.3 Generation of signal

Several techniques exist when it comes to generate the transmitted signal. Signal generation can be passive or active. It can also be digital or analog. We do not cover details in this thesis but the reader can find several references in this interesting topic. Figure 5.2 describes the passive method of producing a compressed signal. This method is defined as passive because a specific filter is used to produce the frequency modulation from a basic rectangular pulse. The MRR radar uses digital computation. The use of digital calculation allows to store several pulses in a memory bank and to select a given pulse at any given instant according to the situation. Indeed, compressed pulses have specific characteristics that have a direct impact on the overall radar performance. For instance, pulse duration T and τ impacts the covered range or the range discriminator ; the frequency drift Δf has an impact on the Doppler filtering and can also be selected.

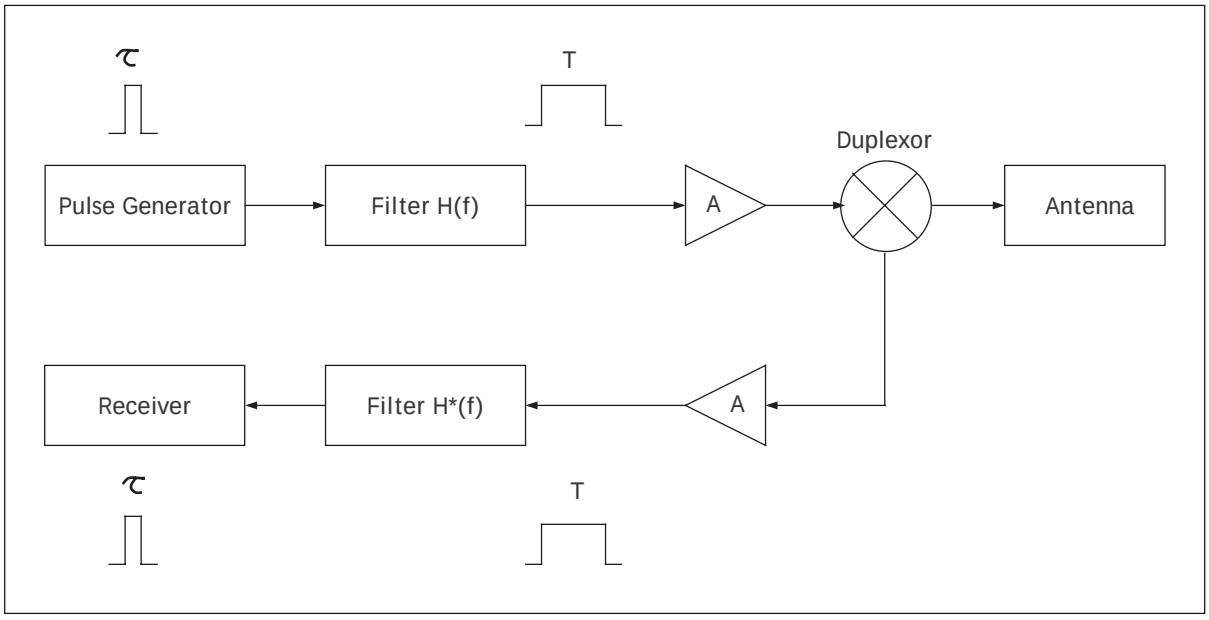

Figure 5.2: Pulse Compression signal generation

5.4 Chirp Signal: Mathematical Approach

The chirp signal is a signal where the instantaneous frequency linearly varies within the duration T of the transmitted pulse. We define the phase variation rate in $[rad/s]$ as $\mu = \frac{2\pi\Delta f}{T}$ and we build the signal $x(t)$ as follow:

$$x(t) = \cos\left(\omega_0 t + \frac{1}{2}\mu t^2\right), \ -\frac{T}{2} \leq t \leq \frac{T}{2} \tag{5.2}$$

where ω_0 is the carrier frequency of the transmitted signal. Its spectrum is computed using the Fourier Transform as:

$$\begin{aligned} X(f) &= FT\{x(t)\} \\ &= \int_{-\frac{T}{2}}^{\frac{T}{2}} \cos\left(\omega_0 t + \frac{1}{2}\mu t^2\right) \exp\left(-j2\pi f t\right) dt. \end{aligned} \tag{5.3}$$

After calculations [Tho82], we obtain:

$$X(f) = \frac{1}{2}\sqrt{\frac{\pi}{\mu}} \exp\left(-\frac{j\left(\omega_0 - \omega\right)^2}{2\mu}\right) \left[C\left(x_1\right) + jS\left(x_1\right) + C\left(x_2\right) + jS\left(x_2\right)\right], \tag{5.4}$$

where

$$x_1 = \frac{\frac{\mu T}{2} + (\omega_0 - \omega)}{\sqrt{\pi\mu}},$$

$$x_2 = \frac{\frac{\mu T}{2} - (\omega_0 - \omega)}{\sqrt{\pi\mu}},$$

$$C(x) = \int_0^x \cos\left(\frac{\pi}{2}y^2\right) dy, \tag{5.5}$$

$$S(x) = \int_0^x \sin\left(\frac{\pi}{2}y^2\right) dy. \tag{5.6}$$

Integrals $C(x)$ and $S(x)$ are called Fresnel integrals. Using the fact that the signal is composed of successive pulses transmitted every $T_R = \frac{1}{F_R}$, the signal spectrum is a discontinuous spectrum composed of regularly spaced narrow rays (every F_R in the frequency domain). The spectrum envelope module is given by [Tho82]:

$$|X(f)| = \frac{1}{2}\sqrt{\frac{\pi}{\mu}} \left[\left(C\left(x_1\right) + C\left(x_2\right)\right)^2 + \left(S\left(x_1\right) + S\left(x_2\right)\right)^2\right]. \tag{5.7}$$

It is possible to show [Tho82, p. 213] that for $\rho = \frac{T}{\tau} = T \times \Delta f$, the envelope module is approximately constant within the considered bandwidth Δf:

$$|X(f)|_{T\times\Delta f >> 1} \cong \sqrt{\frac{\pi}{\mu}},\ f_0 - \frac{\Delta f}{2} \leq t \leq f0 + \frac{\Delta f}{2}. \tag{5.8}$$

In a realistic scenario, it is necessary to consider a complex signal as the noise is modeled as complex. It affects both amplitude and phase.

$$x(t) = \exp\left(j\left(\omega_0 t + \frac{1}{2}\mu t^2\right)\right),\ -\frac{T}{2} \leq t \leq \frac{T}{2}. \tag{5.9}$$

Hence, the transmitted pulse train signal, composed of N_p pulses, is written as:

$$x_{TX} = \sum_{i=0}^{N_p} x\left(t - iT\right). \tag{5.10}$$

5.5 Reception of signal

5.5.1 Matched filter

As any signal transmitted over the air, the chirp signal encounters noise in its two way trip from the transmitted antenna to the target and back to the antenna. In order to maximize the signal-to-noise ratio at the receiving stage, the matched filter is the optimal solution[3] Here we give a summarized overview. For a received signal $y(t)$ which is a time-shifted (delayed) replica of the transmitted signal with additive noise n(t):

$$y(t) = x(t - t_0) + n(t). \tag{5.11}$$

North [D.O63] showed that the frequency response function of the linear, time-invariant filter which maximize the output peak-signal-to-mean-noise (power) ratio for a given input signal-to-noise ratio is given by:

$$H(f) = G_a Y^*(f) \exp(-j2\pi f t_0), \tag{5.12}$$

where:

- $Y(f)$ is the Fourier transform of y(t): $Y(f) = \int_{-\infty}^{+\infty} y(t) \exp(-j2\pi f t) dt$
- t_0: fixed value of time at which the signal is oberved to be maximum (equals the round trip delay of the transmitted signal)
- G_a: filter gain (generally set to unity)

The noise that accompanies the signal is assumed to be stationary and to have a uniform spectrum (white noise). It does not need to be Gaussian. If the noise is not white, then equation (5.12) needs to be rewritten as explained in the next subsection.
In the time domain, using inverse Fourier transform, the matched filter impulse response can be expressed as follow using the fact that $Y^*(f) = Y(-f)$:

$$\begin{aligned} h(t) &= \int_{-\infty}^{+\infty} H(f) \exp j2\pi f t \, df \\ &= G_a \int_{-\infty}^{+\infty} Y^*(f) \exp\left[-j2\pi f \left(t_0 - t\right)\right] df \\ &= G_a \int_{-\infty}^{+\infty} Y(f) \exp\left[j2\pi f \left(t_0 - t\right)\right] df \\ &= G_a \cdot y(t_0 - t) \end{aligned} \tag{5.13}$$

The impulse response of the matched filter is simply the image of the received signal; that is, it is the same as the received signal but run backward in time starting from instant t_0. However, since the noise $n(t)$ is an unknown signal, the filter is matched to the transmitted signal $x(t)$:

$$h(t) = G_a \cdot x(t_0 - t) \tag{5.14}$$

[3] www.wikipedia.com provides a good introduction to the matched filter technique

The output of the matched-filter is expressed as the convolution in the time domain of the received signal with the matched-filter impulse response:

$$\begin{aligned} s(t) &= \int_{-\infty}^{+\infty} y(\tau) \cdot h(t-\tau)\, d\tau \qquad (5.15) \\ &= \int_{-\infty}^{+\infty} (x(\tau) + n(\tau)) \cdot x(t_0 - t - \tau)\, d\tau \\ &= \int_{-\infty}^{+\infty} x(\tau) \cdot x(t_0 - t - \tau)\, d\tau + \int_{-\infty}^{+\infty} n(\tau) \cdot x(t_0 - t - \tau)\, d\tau \\ &= z(t) + w(t) \qquad (5.16) \end{aligned}$$

where $z(t)$ represents the noise-free output from the matched filter and $w(t)$ represents the filtered noise. Note that since the transmitted signal spans a wide frequency range, the matched filter cuts out some signal as well as some background noise since it has a limited bandwidth (equation (4.14)).
In radar signal theory, the matched filter output is affected by the Doppler effect. The apriori unknown frequency shift introduced by the Doppler effect can also be seen in the time domain as an additional def, say t_D. Therefore, since both target range and target Doppler shift are unknown to the system, a bank of matched filters is used to determine the overall delay. Doppler filtering output, i.e. a frequency shift, helps to best estimate the target range by substracting the delay t_D to the total delay.

5.5.2 Matched filter for non-white noise

Equation (5.12) assumes that the noise has a spectrum that is independant of frequency (constant). If this assumption is not true, then the filter that maximizes the output SNR is different. It has been showed in [LR52] that the matched filter frequency response in such situation could be derived as follow:

$$\begin{aligned} H(f) &= \frac{G_a Y^*(f) \exp(-j2\pi f t_0)}{[N_i(f)]^2} \\ &= \frac{1}{N_i(f)} \times G_a \left(\frac{Y^(f)}{N_i(f)} \right)^* \exp(-j2\pi f t_0) \qquad (5.17) \end{aligned}$$

where $N_i(f)$ denotes the noise spectrum.
This indicates that the non-white noise matched filter can be considered as the cascade of two filters. The first filter, with frequency-response function $1/N_i(f)$, acts to make the noise spectrum uniform, or white. It is sometimes called the *whithening filter*. The second is the matched filter described by equation (5.12) when the input is white noise and a input signal with spectrum $S(f)/N_i(f)$.

5.5.3 Issues

At the receiving stage, the signal power is very weak compared to the noise power. The incoming echo signals are first mixed into an Intermediate-Frequency box so that the signal gets shifted to a lower frequency where digital signal processing techniques are achievable. A

sharp bandpass filter centered on the carrier frequency in use eliminates out of band noise. In the military domain, a frequency hopping scheme is used in order to avoid frequency jamming issues.
Figure 5.3 shows the output of the matched filter in a noise free scenario. As noise is a complex process, it distords both signal amplitude and phase. Thus, the main lobe amplitude and position that leads to the target position are affected by the noise. The upper-left figure depicts the real part of a chirp signal (the signal is symetric compared with $t = 0$ axis). We can see how the frequency increases along with the time. The upper-right picture shows the spectrum of the complex chirp signal. The lower figures show the output of the matched filter first in absolute scale and then in dB. Two important parameters has to be taken into account in the figures:

- main lobe width: it defines how accurate the range of a target can be determinated
- sidelobes relative amplitude level: it affects other targets of being shadowed by the matched-filtered output signal

Without any specific signal processing, it appears that the main lobe has an *acceptable*[4] width. The more narrow the main lobe width can be, the better the accuracy of the radar. Concerning sidelobes, the figures show that they have a relatively high amplitude level (an exact value would be -13.2 dB relative to the main lobe magnitude). This is obviously a too high value if we consider that several targets can be detected at the same time. If so, they might be hidden by the sidelobes if they are located in the same direction.
There exists some mathematical techniques that allow to modify main lobe width and sidelobes relative amplitude. These functions are filtering techniques and are called *weighting functions*[5].

5.5.4 Weighting window functions

Let us consider a noise-free scenario. The compressed pulse has a spectrum denoted $X(f)$. This spectrum is fed to a band-limited filter $H(f)$, see figure 5.2, that produces a pulse $x_T(t)$ of duration T and spectrum $X_T(f)$. Since the filter $H(f)$ cuts out some frequencies, the output from the matched filter differs from the original signal $x_T(t)$. It is not a rectangular *chirp* signal of duration T. It is a signal of carrier frequency f_0 that is modulated by a sinusoide. We can express the output as follow:

$$\begin{aligned} x(t) &= \int_{-\infty}^{+\infty} X_T(f) \exp(j2\pi ft) dt \\ &= \sqrt{T\Delta f}\, \frac{\sin \pi \Delta f t}{\pi \Delta f t} \sin(2\pi f_0 t + \phi) \end{aligned} \tag{5.18}$$

where $X_T(f)$ is the filter used to produce the signal of duration T from a pulse of duration τ as depicted in figure 5.2. We can see from figure 5.3 that the output from an uniform (non-weighted) matched filter presents some characteristics that might lower the overall system performance. Indeed, the hight sidelobes level are likely to hide targets. Such a situation is unaccpetable in a military environment.
Weighting functions are here used to compromise between main lobe width and sidelobes relative magnitude. Numerous weighting functions exist with different impact on each parameter. They are mainly used in the frequency domain where bandwidth limitation

[4] It obviously depends on the definition of the term *acceptable*
[5] Sometimes refered as *windowing functions*

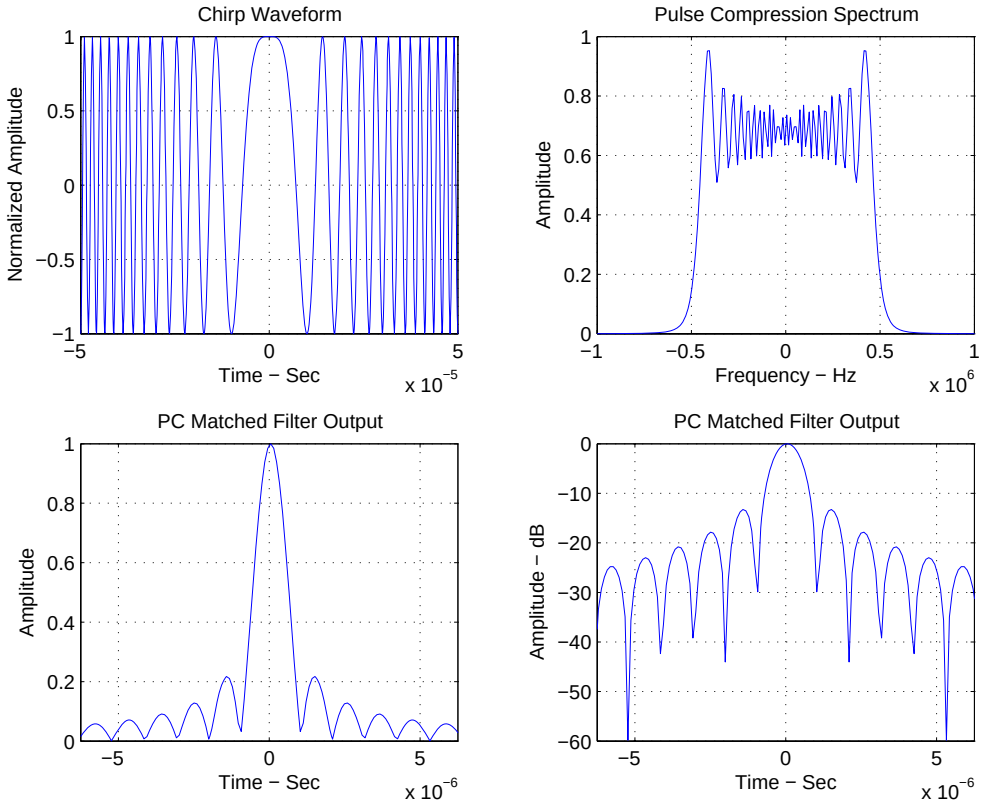

Figure 5.3: Pulse Compression matched filter output

plays an important role. These functions are used in the same manner in the time domain to lower sidelobes relative amplitude and main lobe width. It appears that radar designers have to face a dilemma because a better performance in term of main lobe width can only be achieved at the expense of higher sidelobes amplitude. Figure 5.4 depicts the output of a compressed pulse matched filter. Windowing functions are used to modify time domain characteristics, they are implemented using digital filtering techniques (FIR filters). These filters are placed right after the matched filter.[6]

- Uniform: $\forall k \in [0, N]\,,\ w(k) = 1$
- Hamming: $\forall k \in [0, N]\,,\ w(k) = 0.54 + 0.46\cos\left(2\pi\frac{k}{N}\right)$
- Hanning: $\forall k \in [0, N]\,,\ w(k) = 0.5\left(1 + \cos\left(2\pi\frac{k}{N}\right)\right)$
- Blackman: $\forall k \in [0, N]\,,\ w(k) = 0.42 + 0.5\cos\left(2\pi\frac{k}{N}\right) + 0.08\cos\left(2\pi\frac{2k}{N}\right)$

[6]It can be placed at any other point in the receiving chain as in the frequency domain it comes $X_1(f) \times X_2(f) = X_2(f) \times X_1(f)$

We can see from figure 5.4 that it is possible to achieve great performance in minimizing sidelobes amplitude. Blackman function presents almost -85 dB for its sidelobes relative level but produces an *unacceptable* main lobe width. Most of the modern radars implement Hamming or Hanning window functions because they provide the best trade-off between main lobe width and sidelobes relative amplitude. Depending on the situation, adaptive windowing can be performed in order to select the best weighting function.

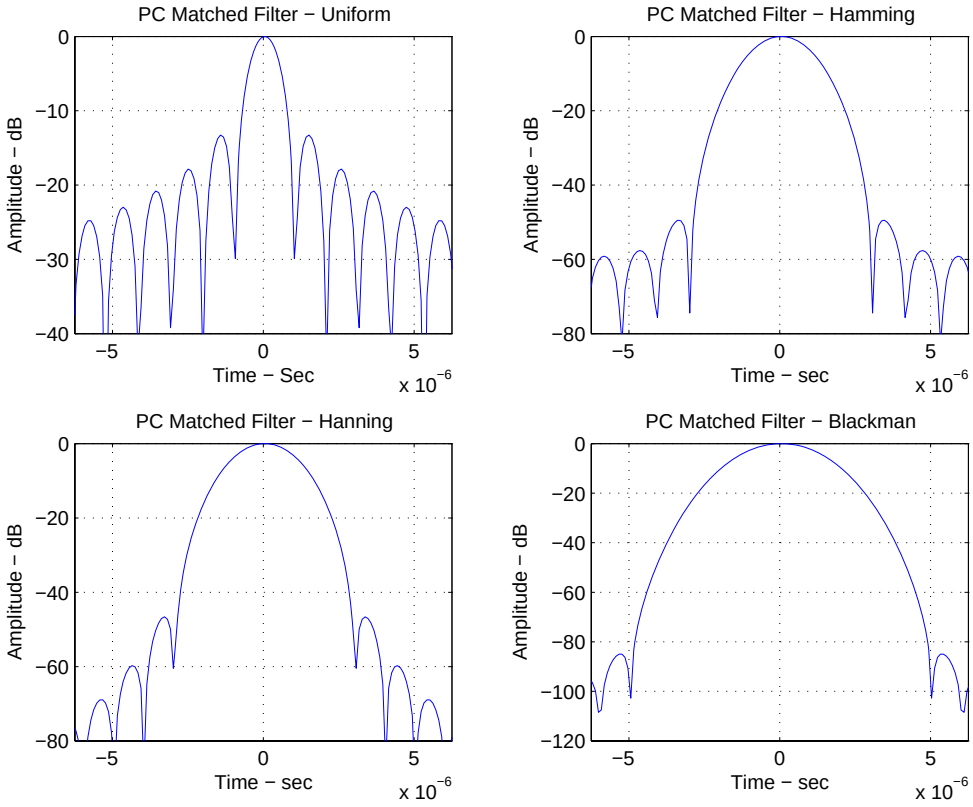

Figure 5.4: Windowing functions examples

5.6 Ambiguity diagram

The radar ambiguity diagram represents the response of the match filter to the signal to which it is matched as well as to doppler-frequency-shifted (mismatched) signals. Since doppler shift and range are canonical conjugate variables there exists an uncertaintly relation between them. It provides a practical way of selecting waveforms for various applications. The output of the matched filter was shown to be equal to the cross-correlation between the received signal and the transmitted signal (equation 5.15). For the ambiguity diagram, only the noise-free component is considered. The ambiguity function is a two-parameters function $\chi(t_0, f_d)$. In [Sko80, p. 411-420], a derivation of the ambiguity function is given.

Basically, the ambiguity function can be calculated in both time and frequency domain.

$$\chi(t_0, f_d) = \int_{-\infty}^{+\infty} x^*(t) x(t - t_0) e^{j2\pi f_d t} dt \tag{5.19}$$

$$\chi(t_0, f_d) = \int_{-\infty}^{+\infty} X^*(f) X(f - f_d) e^{j2\pi f t_0} df \tag{5.20}$$

The ambiguity diagram is obtained by squaring the ambiguity function.

$$A(t_0, f_d) = |\chi(t_0, f_d)|^2 \tag{5.21}$$

For a chirp signal with parameters Δf and T, the ambiguity diagram is expressed as follow.

$$A(t_0, f_d) = rect\left(\frac{t_0}{2T}\right)\left(\frac{T - t_0}{T}\frac{\sin(\pi(\alpha t_0 + f_d)(T - |t_0|))}{\pi(\alpha t_0 + f_d)(T - |t_0|)}\right)^2, \ \alpha = \frac{\Delta f}{T} \tag{5.22}$$

where

$$rect\left(\frac{t_0}{2T}\right) = \begin{cases} 1 & if \quad t_0 \in [-T, T] \\ 0 & otherwise \end{cases} \tag{5.23}$$

This kind of ambiguity diagram is called the knife-edge diagram as it has the shape of a knife edge. Figure 5.5 shows the diagam. The slope of the diagram is equal to the slope of the function depicted in figure 5.1.
The surface delimited by the non-zero part of the diagram defines the two dimensions ambiguity region where it is impossible to determine the echo response. It is not possible to accurately determine the delay t_0 and the Doppler shift f_d. The ideal but unattainable ambiguity diagram would be a single peak of infinitesimal thickness. This ideal model provides ambiguity-free decision as it is not affected by Doppler shift and delay.
For the chirp signal, a solution to decrease the ambiguity is to use alternatively positive and negative slopes. Thus, it reduces the ambiguity region because if we overlap both ambiguity diagrams (positive and negative slope), there is only a limited common region centered around the origin that remains. This leads to less ambiguity.

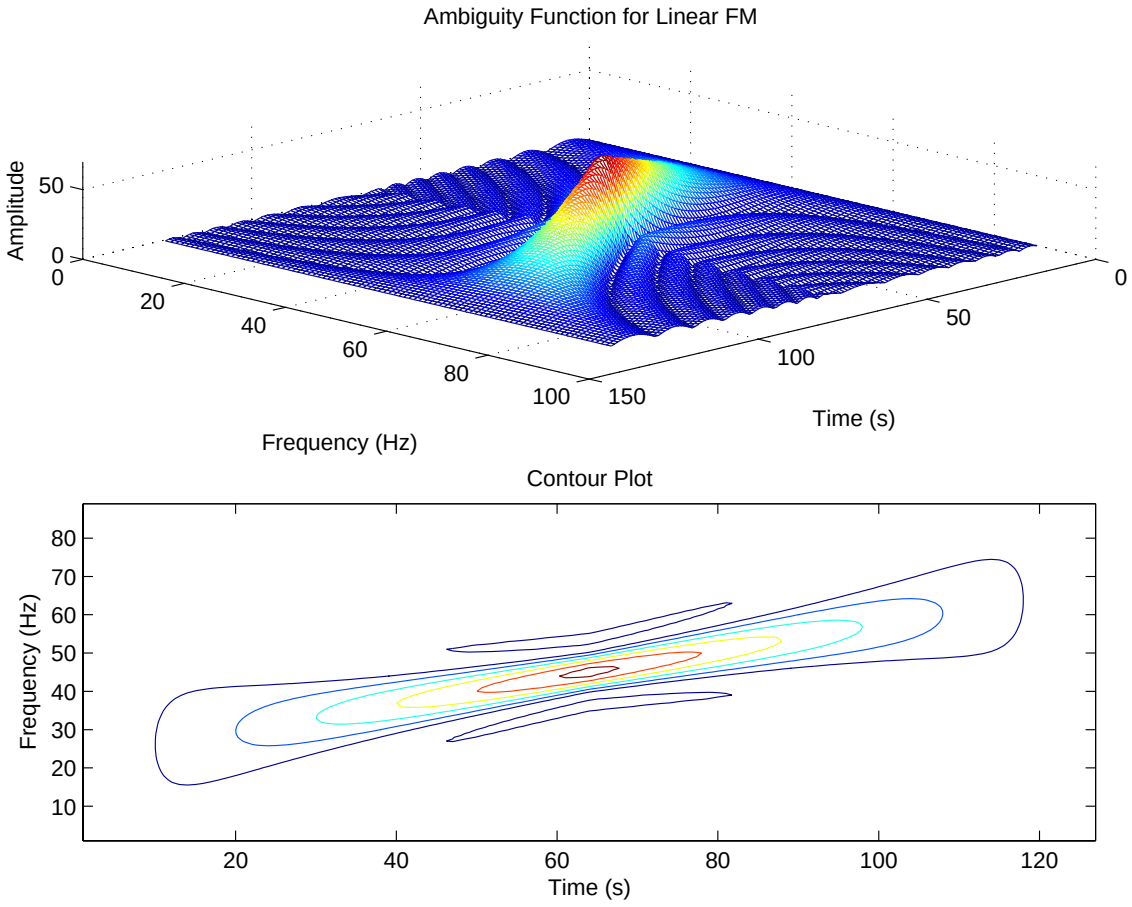

Figure 5.5: Chirp Ambiguity Diagram

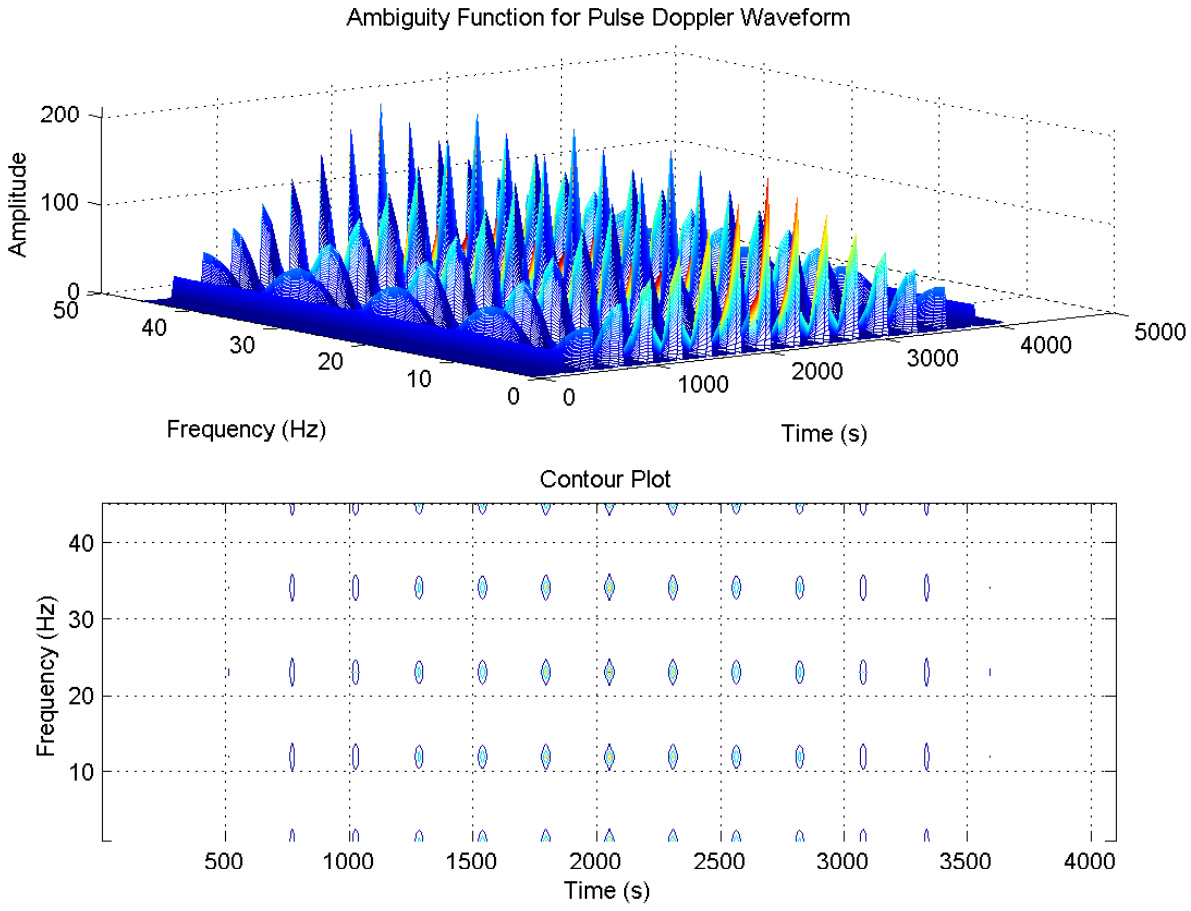

Figure 5.6: Pulse Train Ambiguity Diagram

Chapter 6

Envelope treatment

6.1 Objectives

At this stage of the signal processing chain, the output of the pulse compression box is a noisy complex signal with a wide range of amplitude values. It presents a high peak-to-mean value. This wide range of values may affect the probability of false alarm, and thus system performance. It can decrease radar target detection capability. Very high or very low signal values (due to peaky noise or deep fading) downgrade false alarm performance by generating wrong decisions. Moreover, the antenna gain does not have a constant value within the beamwidth. Maximum gain is obtained at the center and low values occur at the edge of the beam. This leads to a sample-by-sample amplitude modulation (envelope modulation) as the antenna rotates.
In a military scenario it is a priority and a necessity to keep the false alarm rate to the optimum value. Indeed a false alarm can occur in two type of situations:

- if the received signal is high but mainly due to a high noise positive value, it requires to allocate force ressources to an unexisting target and a pure waist of attacking forces
- if the received signal is low but mainly due to a low noise negative value, it causes a target miss, leading to possible severe damages

One signal processing technique that is easy to implement is to select a set of samples, denoted S. The amplitude mean, denoted μ_S, for the sample set S is computed[1]. For each sample x_n in the set S, the magnitude $|x_n|$ is also computed. Then, the difference $\Delta = |\mu_S - |x_n||$ is compared to a threshold ϵ. If $\Delta > \epsilon$, the value of the sample x_n is replaced by a subsitute value x_0.

6.2 Algorithms

Given a transmitted signal composed of N_p consecutive pulses, each pulse is sampled at a rate such that $F_s = 1/T_s$. Recall that within a pulse train, pulses are evenly spaced in time

[1]It is common to discard the maximum and the minimum amplitude value in the set S before computing the mean μ_S

by $T_R = 1/F_R$ seconds. Thus, we can consider the received signal at the output of the pulse compression box as a $(N_p \times T_R F_s)$ matrix. Each row represents a pulse in the pulse train and each column contains samples from all pulses having the same rank within the pulse. The antenna gain is considered approximatively constant during a pulse duration. Samples within a pulse are equaly amplified. Each sample magnitude is compared to the mean of the magnitudes computed over the pulse length. This obviously requires to store data and to wait until the whole pulse ($T_R F_s$ samples) is received. The set is composed of all samples within a pulse.

$$\forall n \in [1, T_R F_s] \text{ if } |x_n| - \frac{1}{T_R F_s} \sum_{n=1}^{T_R F_s} |x_n| > \epsilon_1 \ , \ x_n = x_0 \in R. \tag{6.1}$$

Equation (6.1) basically allows the system to discard high or low signal values that might distort detection performance.
Using the same idea, an algorithm performs a test on the whole pulse train. Here the set is composed of samples having the same rank within the pulse. The set has N_p samples. In this situation, the whole transmitted signal (N_p pulses) must be stored before computing the means.

$$\forall n \in [1, T_R F_s] \text{ if } |x_n| - \frac{1}{N_p} \sum_{n=1}^{N_p} |x_n| > \epsilon_2 \ , \ x_n = x_0 \in R. \tag{6.2}$$

The substitution value x_0 is selected to be a real value in order to *not* disturb Doppler filtering. A complex value modifies the phase of the signal and thus, Doppler filtering is distorted. Thresholds ϵ_1 and ϵ_2 are carrefully chosen as they play an important role in target detection.

Chapter 7

Doppler filtering

7.1 Principle and Method

In the military domain, it is important to be able to evaluate the opponent speed in order to prepare for eventual attacks. It gives very usefull information for strategic manoeuvres. Pulsed-Doppler radar as the name indicates, is capable of evaluating the speed of a target. In fact, in case of a mobile radar (embedded in an aircraft or a ship), it evaluates the target *relative* speed and more precisely, the relative *radial* component of its speed/velocity vector. Let us define a target with speed vector $\vec{v}$ located at a range R from the radar. The target lies on a circle with radius R and centered on the radar position O. Thus, the speed vector $\vec{v}$ can be decomposed as $\vec{v} = \vec{v_r} + \vec{v_t}$. Element $\vec{v_r}$ points from the target to the radar. Element $\vec{v_t}$ is perpendicular to $\vec{v_r}$. Figure 7.1 depicts the situation. According to equation (4.16), the frequency shift of a signal is directly proportional to the absolute value of the vector $\vec{v_r}$. Now, let us imagine a situation where the target moves in circle around the radar. Here, the speed vector is expressed as $\vec{v} = \vec{v_r} + \vec{v_t} = \vec{v_t}$. The target does not encounter Doppler effect although is it moving. However, a solution to this problem exists.
As expressed earlier in this paper, two techniques allow to evaluate the target speed:

- direct: using the Doppler effect and appropriate filters (generally a bank of digital FIR filters)
- indirect: using successive evaluations of the target range and antenna pointing direction (interpolation)

In the MRR radar, the *direct* method is used. It is the most popular as it does not require any memory to store values and nowadays, state-of-the-art DSP software and hardware allow very fast computations. The bank of filters is composed of several evenly spaced and overlapping FIR narrow-band filters with cut-off frequency centered around desired Doppler shifts. Recall that a Doppler shift in the frequency domain is directly proportional in the speed domain to the radial velocity of the target (equation (4.16)). The fact that the filter frequency responses are overlapping avoids gaps in the considered range of Doppler shifts. Thus a target *hit* is likely to occur in two filters *but* at different amplitudes. The most used technique is the so-called MTI-MTD. A short demonstration is illustrated in [CCHF00]. The MTI is basically a FFT processor which output gives information on the presence (or not) of target. Thus, the bank of filters operates via FFT. An amplitude threshold is used to determine whether or not targets are present. If not, the MTD is skipped. If at least one

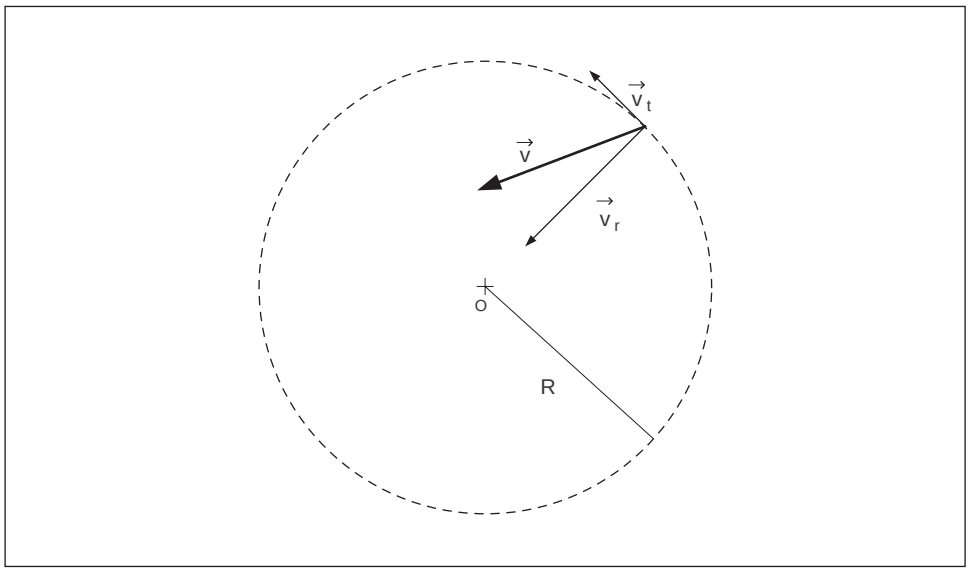

Figure 7.1: Speed vector decomposition

target is present in the pointed direction, the MTD process the data to find out about the target moving direction (away or toward from the radar). It can also evaluate the target range if the radar does not use pulse compression technique. It may also be used as a help to improve pulse compression accuracy.

7.2 Module and Logarithm

At the output of the Doppler filtering stage, the signal is in a complex format, i.e. $x = \rho e^{i\theta}$. However, the phase θ of the signal is not of importance anymore for the rest of the signal processing chain. Thus, we can compute the module ρ_n for each sample x_n such that:

$$\rho_n = |x_n| = \sqrt{(Re(x_n))^2 + (Im(x_n))^2}. \tag{7.1}$$

Then, for each sample, we compute the logarithm of the module we have just calculated. The main reasons for computing the logarithm are:

- range of values is decreased, this permits to increase accuracy in the number representation; this have a direct impact on the overall radar performance,
- statistic properties of the output signal are modified because logarithm is not a linear operator; this is the main reason why it is used because the output signal has a variance that is independant of the input signal, i.e. it is constant.

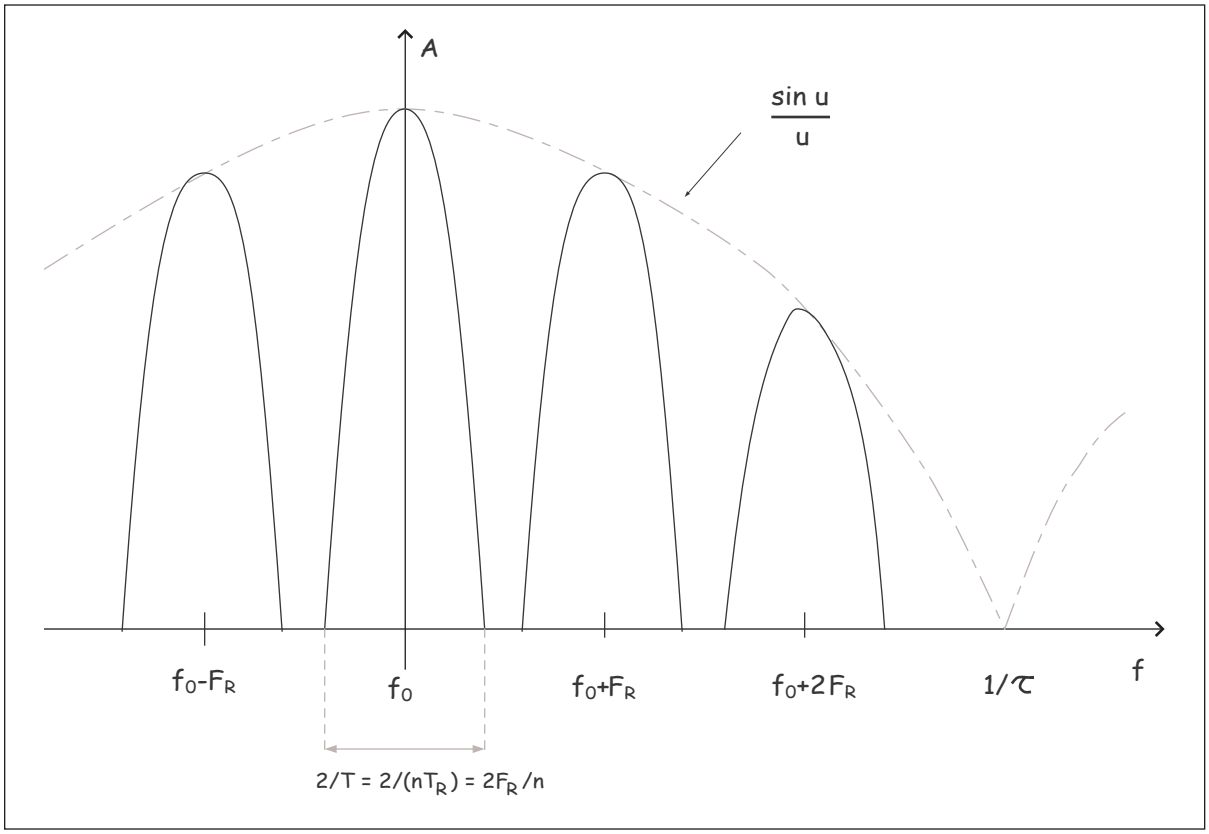

Figure 7.2: Train Pulses Spectrum

Let a logarithmic detector have the following transfer function $y = a \log(bx)$ where parameters $(a, b) \in R$. Let x be the input complex signal which module has a circular probability[1] function $p_x(x)$.

$$p_x(x) = \frac{2x}{\sigma^2} \exp\left(\frac{-x^2}{\sigma^2}\right). \tag{7.2}$$

We set the following variable substitution $u = \frac{x^2}{\sigma^2}$.

$$du = \frac{2x}{\sigma^2} dx,$$

and

$$p_x(u)du = e^{-u}du.$$

[1]The Rayleigh probability model is used as the noise is modeled as complex AWGN

The transfer function can be rewritten as:

$$y = a\log(bx) = \frac{a}{2}\log\left(b^2x^2\right) = \frac{a}{2}\left[\log\left(b^2\sigma^2\right) + \log u\right], \tag{7.3}$$

$$\begin{aligned} E\{y\} &= \int_{-\infty}^{+\infty} \frac{a}{2}\left[\log\left(b^2\sigma^2\right) + \log u\right] p(u)du \\ &= \frac{a}{2}\left[\log\left(b^2\sigma^2\right) + \int_0^{+\infty} \log(u)p(u)du\right], \end{aligned} \tag{7.4}$$

since

$$\int_0^{+\infty} p(u)du = 1,$$

$$\begin{aligned} E\left\{y^2\right\} &= \int_0^{+\infty} \frac{a^2}{4}\left[\log\left(b^2\sigma^2\right) + \log u\right]^2 p(u)du \\ &= \frac{a^2}{4}\left[\left(\log\left(b^2\sigma^2\right)\right)^2 + 2\log\left(b^2\sigma^2\right)\int_0^{+\infty}\log(u)p(u)du + \int_0^{+\infty}\left(\log(u)\right)^2 p(u)du\right]. \end{aligned} \tag{7.5}$$

If we combine equation (7.4) and equation (7.5) to compute the variance, it comes:

$$var(y) = E\left\{y^2\right\} - \left[E\{y\}\right]^2, \tag{7.6}$$

$$\begin{aligned} var(y) &= \frac{a^2}{4}\left[\int_0^{+\infty}\left(\log(u)\right)^2 p(u)du - \left(\int_0^{+\infty}\log(u)p(u)du\right)^2\right] \\ &= \frac{a^2}{4}\left[\int_0^{+\infty}\left(\log(u)\right)^2 e^{-u}du - \left(\int_0^{+\infty}\log(u)e^{-u}du\right)^2\right]. \end{aligned} \tag{7.7}$$

Using some basic calculations, we obtain:

$$var(y) = \frac{a^2}{4}\frac{\pi^2}{6}. \tag{7.8}$$

In fact, we cannot have such a transfer function because a pure logarithmic function outputs minus infinity when its input is equal to zero ($\log x_{x=0} = -\infty$). A slightly modified transfer function - more realistic - is used and the result remain the same as the modified function can be approximated as a pure logarithmic.

7.3 Static Target elimination

Doppler filtering uses frequency discrimination to distinguish between targets. The received signal contains echo signals from various targets as well as signals corresponding to different noise sources. Moving target and static (non-moving) targets are treated in a different fashion. Although a target is not moving, it backscatters an echo which is recognized by

the signal processing chain embedded on the radar. Indeed, each type of target is assigned a specific *signature*, that is the RCS parameter. It allows to differentiate bewteen static target echo and environment echos. Echos from the environment, and especially from the ground or the sea are sufficiently strong to cause close moving targets to be unseen from the radar if not processed efficiently. These signals have relatively strong magnitude but they do not generate Doppler effect since they are produced by static scatters. Thus, they can be easily discriminated by their Doppler effect from scan to scan. Equation (7.9) expresses the frequency model of static clutter. It appears that the clutter is not exactly Doppler effect free but the signal energy is mainly focused around the carrier frequency f_0.

$$X(f) = k \exp\left(-a\left(\frac{f}{f_0}\right)^2\right) \quad f \in [0, F_R]\,,\ k \in R,\ a \in \left[10^{14}, 10^{18}\right]. \tag{7.9}$$

The technique used to eliminate such undesirable echos employs a FIR filter that has the following characteristics:

- flat amplitude/frequency response in the range $[0, F_R]$
- null amplitude at frequencies such that $f = k \times F_R$, $k \in Z$

This technique is also called the MTI. It uses a velocity discrimnation factor. Such *ideal* filter does not exist and an approximate solution is adopted through so-called single canceler or double canceler. These techniques use basic computation in order to cancel out static echo signal. The canceling technique slightly differs whether we assume a single or a double cancellation.

- single cancellation: here, the received signal is fed to a direct path and to a delay box of value T_R so that the output $y(t)_{sc}$ can be viewed as :

  $$y(t)_{sc} = x(t) - x(t - T_R)$$

- double cancellation: here, two consecutive delay boxes are used so that the final output $y(t)_{dc}$ can be viewed as:

  $$y(t)_{dc} = y(t)_{sc} - y(t - T_R)_{sc} = x(t) - 2x(t - T_R) + x(t - 2T_R)$$

  Thus the output can be understood as the difference between a delayed version of the output from a single canceller and the output from a single canceler.

The following equation expresse the output of a single canceller and the output for a double canceller.

$$|y(t)_{sc}| = 2\sin\left(\frac{\pi f_d}{F_R}\right)\ \sin\left(t\frac{2\pi f_d}{F_R} + \phi\right), \tag{7.10}$$

$$|y(t)_{dc}| = 4\sin^2\left(\frac{\pi f_d}{F_R}\right)\ \cos\left(t\frac{2\pi f_d}{F_R} + \phi\right), \tag{7.11}$$

where ϕ is a random angle that introduces *blind phases* phenomena. The outputs from the cancellers are null if $\sin(\pi f_d/F_R) = 0$ but they also become zero if the second term is null. This term modulates the magnitude of the filter output. It degrades the probability of detection as it affects the signal amplitude.
A hardware solution to get rid of this blind phases term is depicted in [Tho82, p. 102]. Other filters are also available to produce sharp brickwall-like frequency response. They

have the advantage to avoid the blind phases phenomena but at the cost of more complex computation. A convolution is needed rather than a simple delay box. These filters are FIR low-pass filters with order in the range $2 \leq n \leq 5$. Figure 7.3 shows the frequency response for both single and double cancellation. Blind phase effect is not shown. One question might arise to the reader. These cancellers also remove signal at frequencies multiple of the repetition frequenccy F_R. Thus, any target with a relative radial velocity that would produce a Doppler shift equal to an integer multiple of the repetition frequency F_R is canceled out. This specific speeds are called *blind speeds*. There exists techniques to avoid such a drawback. These techniques modify the repetition frequency on the fly such that a given target does not remain in the blind speed range.

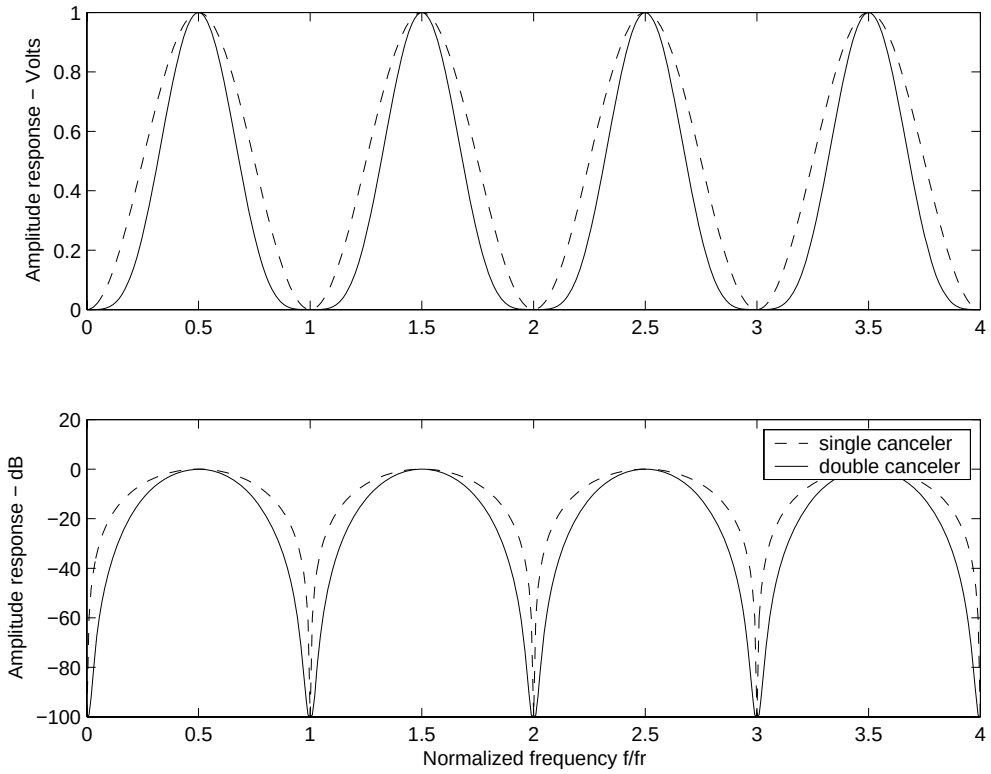

Figure 7.3: Single and Double Cancelers

7.4 Staggering - Wobbulation

7.4.1 Ambiguities

The use of a pulse train instead of a continuous wave or a mono pulse adds in complexity when it comes to target range estimation. Since a given target is likely to reflect echo signals

from several pulses within a pulse train, it is difficult to determine from which transmitted pulse, the received echo signals match. Recall from figure 4.1 that between two consecutive transmitted pulses, there is a duration of T_R seconds. Thus, when an echo signal is received at time instant t_0, the detected signal leads to an estimate of the target range d such that:

$$d = \frac{c}{2}\, t_0 \mod \left(\frac{c}{2}\, T_R\right) \tag{7.12}$$

We say that there is an amiguity of $cT_R/2$ on the range estimate.
On the other hand, there is also an ambiguity in velocity due to a frequency pattern periodicity. Recall that the transmitted signal is pulse-repetition based. Figure 7.2 depicts the frequency representation of the transmitted signal. It composed of rays spaced by F_R hertz. Thus, if the Doppler effect produces a frequency shift f_d such that $f_d \geq F_R/2$, it becomes impossible to find out which ray the Doppler shift belongs to. There is no way to guess if the Doppler shift is larger than $F_R/2$ or less than $F_R/2$. The target velocity estimate can be expressed as:

$$v_r = \frac{\lambda}{2}\, f_d \mod \left(\frac{\lambda}{2}\, F_R\right) \tag{7.13}$$

7.4.2 Resolving ambiguities

A Pulse-Doppler radar faces the so-called Doppler dilema: a good choice of pulse repetion frequency to achieve a large unambiguous range is a poor choice to achieve a large unambiguous velocity. In order to get rid of the ambiguity problem introduced by the Pulse-Doppler radar, an easy-to-implement technique exists. It is based on the modulation of the repetition frequency F_R. In litterature, the technique is called *wobbulation*. The modulation can be continuous or discrete. Most modern radars use the discrete method where the repetition frequency value changes among a set of discrete values.

- For speed ambiguities, as recalled earlier, the signal is a set of evenly spaced rays. The width of the ray is linked to the duration $T = n \times T_R$ of the transmitted signal, where n is the number of pulses within the pulse train. The width of the rays is given as $w = 2/T = 2/\left(n \times T_R\right) = 2F_R/n$. It appears that it is directly proportional to the repetition frequency. Obviously, in order to take into account higher Doppler shifts, one can increase F_R as we have $F_R \geq 2f_d$, i.e. $F_R \geq 4v_{rmax}/\lambda$. This expression gives a way to select the minimum repetition frequency required for a given target speed.

- For range ambiguities, the idea is to increase the maximum ambiguity-free range. It is defined as $d_{amb-free} = cT_R/2$. Here, wobbulation of the repetition frequency solves both the range ambiguity issue and the blind speeds issue. If we define T_b to be the main repetition period, it is possible to define, say two frequencies multiple of the main repetition frequency $F_b = 1/T_b$ such that, $F_1 = n_1 \times F_b$ and $F_2 = n_2 \times F_b$ where $(n_1, n_2) \in N$. If we alternatively use those two repetition frequencies, we can obtain a larger maximum range R_{max} that we would have obtained using only the base repetiton frequency. This maximum ambiguity-free range is given by:

$$R_{max} = \frac{cT_b}{2} = \frac{c}{2F_b} = \frac{cn_1}{2F_{R_1}} = \frac{cn_2}{2F_{R_2}} \tag{7.14}$$

  It is possible to use more than two repetition frequencies. Three multiple frequencies is a common value. It is usual to take n_1, n_2 and n_3 to be three consecutive integers. Moreover, recall that all Doppler shifts such that $f_d = n \times F_R$ designate a blind speed. Thus, wobbulation by the use of different repetition frequencies solves the issue as a given Doppler shift does not remain *blind* after a change in F_R.

Figure 7.4 depicts the wobbulation technique. It shows in the range domain how the use of two repetition frequencies can increase the maximum ambiguity-free range. The final output is depicted in the bottom of the figure. The two repetition frequencies F_{R1} and F_{R2} produce two transmitted signal. These signals are sent alternatively, *not* at the same time. The combination of their respetive echo response allows to extend the maximum range. This technique obviously requires to store the received echo signals and combine them afterward.
Figure 7.5 illustrates the technique from a Doppler shift perspective. It shows how two multiple of the base repetition frequency push away the first blind speed. It also requires to store received signals and combine them.

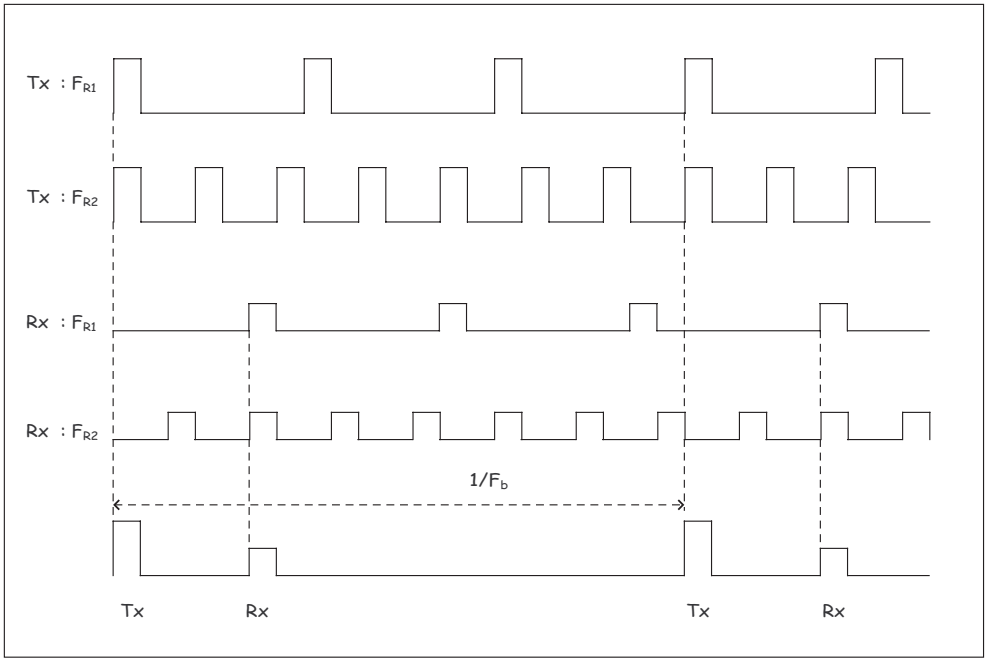

Figure 7.4: Wobbulation technique in the range domain

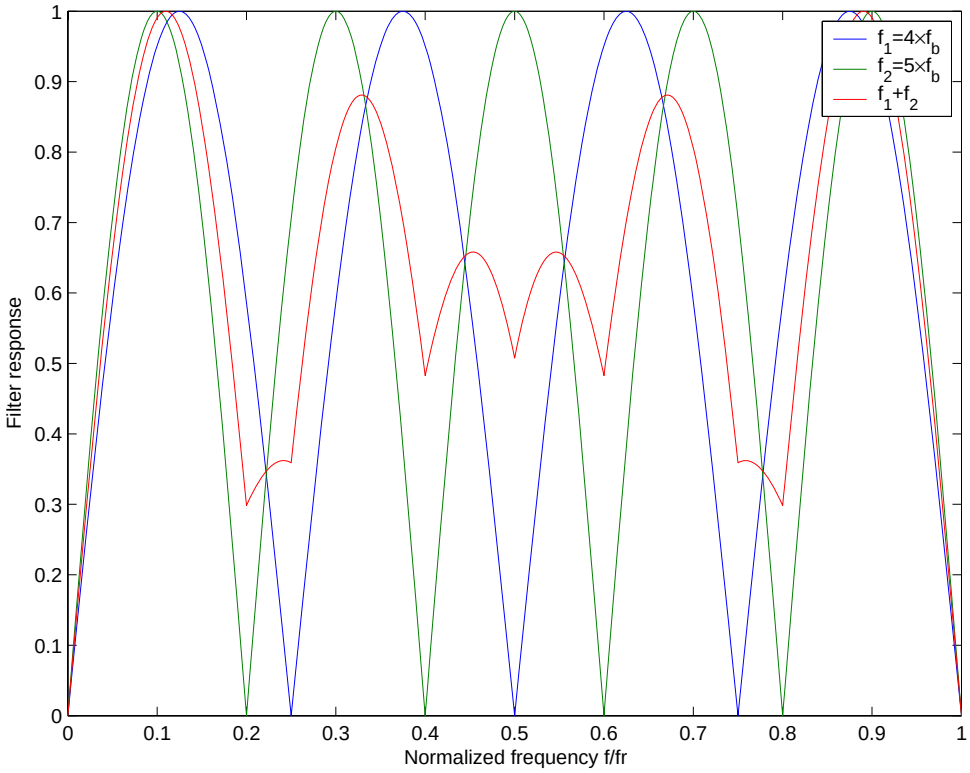

Figure 7.5: Wobbulation technique in the speed domain

Chapter 8

CFAR processors

Received radar signals are affected by various sources of noise. In order to maintain overall detection performance, radar systems have to estimate and evaluate the different noise power. The received signal are then compared to a threshold which is a function of a set of estimates. If the signal exceeds the threshold, detection or at least assumption of detection is performed.
Let us define some basic concepts. Recall that the 3D volume covered by the radar can be seen as superimposed 2D maps. Each 2D map corresponds to one pointing site direction. The MRR radar stores five different maps (surface, low altitude, average altitude, high altitude or very high altitude). Each map is divided in cells according to two criteria:

- step angle $\Delta\theta$: it defines how many angle sectors the map contains
- sampling frequency F_s: it defines the number of cells the map contains in the range dimension.

It is obvious that the maps should have a limited size in order to perform fast calculation and to minimize memory usage. However, the maps need to be accurate enough to represent as close as possible the radar surrounding environment. Some requirements can be stated:

- $N_{sec} > 360/\theta_{3dB}$: the number of sectors should be greater that the ratio between a complete round cycle ($360°$) and the $3dB$ beamwidth angle of the antenna ; this is in order to improve accuracy in the azimuthal (horizontal) plan
- $d_{min} = c/F_s$: the sampling frequency F_s defines the size in $[m]$ of a cell ; it appears that to improve range accuracy, one could increase the sampling frequency but this is obviously at the expense of larger amount of data to handle

Radar signal processing tends accurately distinguish the presence of a target among harmful signal such as thermal noise, clutter and jamming signals. Decision on the *presence of a target* is a probabilistic - stochastic phenomena. When a target is really present , the radar detects it with a certain probability, the probability of detection P_d. When there is no target, there can be a misleading decision of the presence of a target. This is called the probability of false alarm, denoted P_{fa}.
Radars are regulated such that they privilege false alarm. This means that the radar operation is set such that the probability of false alarm does not exceed a given low value, for instance 10^{-6}. This might appear confusing but it is considered more risky to announce

the presence of a target when there is none, than the contrary. If the radar pilots the launch of inter-continetal missiles, this becomes obvious. If the radar drives the opening of a door, then the probability of false alarm can be set to a higher value.
The main task of the CFAR processors is to compute estimates of the different noise power. Most of the time, to describe an environment, its mean level suffices. From this mean level, the threshold is set. Old CFAR processors used to compute the mean μ and the standard deviation σ. Then, the threshold K was set such that:

$$K[dB] = \mu[dB] + n[dB] \text{ , where } n \propto \sigma. \tag{8.1}$$

The environment estimate accuracy is increased as more samples are used in the computation. A loss due to the finite number of samples used in the calculation is introduced by CFAR processors. The loss is inversely proportional to the number of independant samples. The environment can be obtained through calculating the average of either module, squared modules or by taking the logarithmic value of modules. The last solution is the one embedded in the MRR radar. The processor is called a LOGCA-CFAR(LOGarithmic Cell Averaging CFAR). Section 7.2 gives one of the reasons why the logarithmic computation is employed. Another reason is that in order to set the threshold K to a certain level (ndB greater than the computed environment), using modules or squared modules requires to perform a multiplication whereas using logarithm only requires a basic addition. Moreover, if a target is present in the set of cells used to compute the average, the target is *averaged* in dB. This produces a weaker deterioration of the estimate. Averaging modules or averaging squared modules is more sensitive to the presence of target, when a strong signal is present. Other techniques exist to produce an estimate of the environment. Instead of averaging the set of cells, other CFAR processors perform the *greatest of* selection where the maximum value among the set of cell is selected to be the output of the estimator. They are denoted GO-CFAR. The set of reference cells can be selected in different ways. It mainly depends on the spatial properties of the considered clutter. The MRR radar owns three CFAR processors as it can encounter:

- atmospherical clutter and thermal noise
- sea clutter
- ground clutter

Recall that Doppler filtering box outputs several signals: one per filter in the FIR bank of filters[1]. It has been said before that the clutter maps have only two dimensions. In fact, a third dimension is added: the Doppler filter rank. Estimates are computed for a selecton of filters according to the Doppler response of the clutter.
Numerous studies have been conducted on CFAR processors as every radar application requires specific processors according to surrounding environment ([MAK00] emphases on adaptive CFAR, [Wat98] emphases on CFAR for sea clutter).

8.1 Range CFAR

8.1.1 Objectives

The range CFAR aims to combat both thermal noise and front-edge atmospherical clutter. It operates in the range direction with a non-recursive procedure. Estimates are computed

[1] One per central radial speed

in the current antenna scan and directly applied. Two primary average estimates are computed. One is computed over a set of N_{set} cells before the considered cell ; it is denoted μ_ℓ where ℓ stands for left. The other one is computed over N_{set} cells after the considered cell and is denoted μ_r (r here stands for right)[2].

$$\text{if } k \geq N_{est} + N_g,\ \mu_\ell(k) = \frac{1}{N_{est}} \sum_{j=k-(N_{est}+N_g)}^{k-(N_g+1)} \rho_{log}(j), \tag{8.2}$$

$$\text{if } k \leq N_c - (N_{est} + N_g),\ \mu_r(k) = \frac{1}{N_{est}} \sum_{j=k+(N_{est}+N_g)}^{k+(N_g+1)} \rho_{log}(j), \tag{8.3}$$

where ρ_{log} stands for the logarithmic module of each sample, N_c denotes the maximum range in number of cells, N_g defines the number of *guard* cells and N_{est} is the number of cells used to compute the average. Then, for each cell two secondary estimates are computed as follow:

$$\mu_{max} = \max(\mu_\ell, \mu_r), \tag{8.4}$$

$$\mu_{avg} = \frac{1}{2}(\mu_\ell + \mu_r). \tag{8.5}$$

The final output of the estimator is set for each cell using a threshold:

$$\mu_{range} = \begin{cases} \mu_{max} & if\ |\mu_{max} - \mu_{avg}| > \epsilon \\ \mu_{avg} & if\ |\mu_{max} - \mu_{avg}| \leq \epsilon. \end{cases} \tag{8.6}$$

Estimates μ_{max} applies when the clutter is not homogeneous (front edge clutter). Estimate μ_{avg} applies when the clutter is diffuse, homogenous. The threshold ϵ is selected such that the probability to chose μ_{max} instead of μ_{avg} in presence of thermal noise only or in presence of homogeneous clutter is low, for instance 10^{-4}.

8.2 ACP: Anti-Clutter Processors

ACPs tries to best estimate clutter. The MRR radar is designed to be embedded on any frigate. Thus, it must combat both ground and sea clutter. Therefore, it owns two Anti-Clutter Processors. As water and ground do not generate exactly the same echos and do not have the same spatial properties, minors differences appears between sea and ground ACP algorithms.
Ground clutter is not stationnary in range, nor it is stationnary in Doppler (it is Doppler free). Sea clutter is not stationnary in distance and it spans a couple of Doppler filters. The clutter estimates are obtained through a combination of filters. ACP technique uses simple MA(1)[3] [Hay96] filters to determine the clutter power. It is useless to compute the clutter estimate for every single cell, i.e every single sample. Thus, the *clutter power* maps generated by ACP processors employs a different quantum. Ground clutter and sea

[2]Equations (8.2) and (8.3) do not apply over the whole range: at the beginning of the range, only μ_r is valid and at the end of the range, only μ_ℓ

[3]Moving Average of Order 1

clutter power are considered to have the same value within a given set of cells, denoted N_{set}. This cell set is composed of $(N_{range} \times N_{sector})$ cells. The cell set N_{set} is later denoted as a *case*. For each pointed direction, a current sector is defined. The cell set (or case) is centered around this current sector and around the considered cell. Therefore, the clutter 2D maps are of size $\left(N_{sec} \times \frac{R_{max}}{d_{min} \times N_{range}}\right)$ where $\frac{R_{max}}{d_{min}}$ represents the maximum range to be considered by the radar in cells unit.
Using this definition, it appears that during an antenna scan, each cell serves as a considered cell *and* as a neighbouring cell.
Finally, the maps are expanded to their original size. Each case duplicate its value to all the cells in the case but *only* in the range direction (N_{range}).

8.2.1 Sea ACP

Sea clutter presents a peaky amplitude distribution. This might produce false alarm to occur. Therefore, it is necessary to estimate both the mean μ and the variance σ^2 of the sea clutter. MA(1) filters smooth the outputs μ_n and σ_n^2 from scan to scan.
Sea clutter produces some Doppler effect. Therefore, estimates are computed over a couple of Doppler filter, within the range of a few miles per hour.

$$y = \max_{i \in N_{set}} \left(\rho_{log_i}\right),$$

$$\begin{aligned} \sigma_n^2 &= k\sigma_{n-1}^2 + (1-k)\left(\mu_{n-1} - y\right)^2, \\ \mu_n &= k\mu_{n-1} + (1-k)y, \\ \mu_{sea} &= \mu_{n-1} + f\left(\sigma_{n-1}^2\right). \end{aligned} \tag{8.7}$$

Parameter k impacts how fast and how accurately filters converge to their optimal value (steady state). This parameter is adaptative: it changes during radar operation. The function $f(x)$ in equation (8.7) is an experimental function that gives a contant value according to the smoothed sea clutter variance σ_{n-1}^2 computed by the first MA(1) filter on the previous scan. It is used to adjust the clutter estimate. Obvisously, the map have pre-defined value at start up, when $n = 0$ (first scan).

8.2.2 Ground ACP

In the case of ground ACP, the algorithm is slightly different. It also uses a MA(1) filter. The estimate μ_{ground} is also updated with the previously calculated mean value, but in case of ground a constant α is added to the estimate in order to take into account ground material. Ground can be made with grass, rocks, sand.

$$y = \max_{i \in N_{set}} \left(\rho_{log_i}\right),$$

$$\mu_n = k\mu_{n-1} + (1-k)y, \tag{8.8}$$

$$\mu_{ground} = \mu_{n-1} + \alpha. \tag{8.9}$$

In case of ground clutter, the case (set of cells used to compute the max) is made up with two to height cells. It is sometimes referred as short ACP.

8.3 Target Fluctuation: Swerling models

Once the clutter estimates have been performed, the received signal is compared to the threshold K defined in equation (8.1). The threshold is set according to the probability of detection P_d required by the system. The probability of detection is a statistical function which form strongly depends on the target signal response. Recall that targets are classified according to a parameter called the radar cross section (equation (4.11)). Common mean values are listed in table 4.1. RCS parameter has to be taken into account as it reflects how much signal is backscattered by a given target. Statistical models have been designed during the last decades. There exists mainly five models that describe target radar cross-section flucuations. These models are the so-called Swerling models, from I to V. Swerling target models give the RCS of a given object based on the chi-square[4] probability density function, which has the following form:

$$p(\sigma) = \frac{m}{\Gamma(m)\sigma_{av}} \left(\frac{m\sigma}{\sigma_{av}}\right)^{m-1} \exp\left(-\frac{m\sigma}{\sigma_{av}}\right), \tag{8.10}$$

where σ_{av} defines the mean of σ, $2m$ is the degree of freedom and $\Gamma(m)$ is the complete Gamma function. Swerling target models are special cases of the Chi-Square target models with specific degrees of freedom. This degree of freedom is usually an integer value in statistics. In radar theory, $2m$ can be any positive real value. It affects how much fluctuations the target presents ; the larger $2m$ is, the less fluctuations. Is not easy to determine the mean value σ_{av} of the RCS since the target has to be completely defined. For instance, for a sea-based radar, the targets are most likely to be seen from the front, the back or the side but unlikely from the top or the bottom. Therefore, each military force has a bank of pre-defined RCS profiles that it uses as input when it comes to designing a CFAR box in the radar overall system. These profiles are very important as they represent a great help in detecting target. Profiles are also called *signatures*.
An overview of Swerling models is described in ([Joh97]). A mathematical derivation of Swerling models is given in [Swe60].

- Swerling I: here, the RCS varies according to a Chi-square probability density function with two degrees of freedom ($m = 1$). This applies to a target that is made up of many independent scatterers of roughly equal areas. As little as half a few (less than ten) scattering surfaces can produce this distribution. Swerling I describes a target whose radar cross-section is constant throughout a single scan (signal is assumed constant from pulse to pulse whithin the scan), but varies independently from scan to scan.

- Swerling II: here, the RCS is similar to a Swerling-I model except that RCS values vary from pulse to pulse within the scan

- Swerling III: here, the RCS varies according to a Chi-square probability density function with four degrees of freedom ($m = 2$). This model approximates an object with one large scattering surface with several other small scattering surfaces. The RCS values are constant through a single scan.

- Swerling IV: here, the RCS is similar to a Swerling-III model except that RCS values vary from pulse to pulse within the scan

- Swerling V: here, the RCS value is assumed to be constant[5] in time ($m \to +\infty$).

[4] http://mathworld.wolfram.com/Chi-SquaredDistribution.html
[5] Also known as Swerling 0 or Marcum model

In [Swe60], Swerling derives the probability density function for each of the given fluctuations model and shows graphical outputs. Models I and II are the most used in radar systems as they best approximate targets in the aviation domain. In these cases the pdf is given as the probability of a signal to exceed a threshold, the so-called false alarm rate.

$$P_d = \int_K^{+\infty} p(\sigma)\, d\sigma.$$

For a Swerling I models, we have:

$$P_d \approx \left(1 + \frac{1}{n\sigma_{av}}\right)^{n-1} \exp\left(\frac{-K}{n\sigma_{av}}\right), \tag{8.11}$$

and for a Swerling II model, it comes:

$$P_d = 1 - I\left(\frac{K}{(1+\sigma_{av})\sqrt{n}}, n-1\right), \tag{8.12}$$

where K is the threshold, n the number of pulses integrated and σ_{av} the mean value of the signal. The function $I(a,x)$ is the *upper*[6] incomplete Gamma function
The threshold K is set using equation (8.1). Using the outputs of the CFAR processors, the equation can be rewritten as:

$$K[dB] = \max\left(\mu_{range}, \mu_{sea}, \mu_{ground}\right) + n[dB] \tag{8.13}$$

When designing a radar, probablities P_fa and P_d are decided according to strategical requirements. Thus, threshold K becomes a variable of the CFAR processor outputs.
Modern radars do not use such adaptive threshold in order to reduce the computationnal complexity of their systems. Instead, according to the situation (ground, sea) and according to the range (close range, middle range, far range), radar automatically apply constant thresholds. For each cell, the following test is performed to select the most efficient threshold.

$$K = \begin{cases} K_1 & if \max\left(\mu_{range}, \mu_{sea}, \mu_{ground}\right) = \mu_{range} \\ K_2 & if \max\left(\mu_{range}, \mu_{sea}, \mu_{ground}\right) = \mu_{sea} \\ K_2 & if \max\left(\mu_{range}, \mu_{sea}, \mu_{ground}\right) = \mu_{ground} \end{cases} \tag{8.14}$$

[6]There exist two definitions of the incomplete Gamma function: one is named *lower* and the other is named *upper*. The names depends on the variable in the integration boundaries whether it is set as the lower limit or the upper limit. The upper incomplete Gamma function is defined as: $I\left(a,x\right) = \int_x^{+\infty} t^{a-1}e^{-t}dt$

Chapter 9

Post Integration - Sliding Post Integration

9.1 Objectives

The objective of the post-integration is to use the advantage of multi-pulse transmission. Each pulse concentrates a certain amount of energy that it is important to capture. The process of integration sums up the pulses in order to maximize the signal-to-noise ratio. The summation can be done in a coherent fashion or not. If we consider that a radar has a revolution cycle time speed of N round per minute and a pulse repetition frequency denoted F_R, and if we consider that the antenna has a $3dB$ beamwidth denoted $\theta 3dB$, thus the number of pulses per echo (backscattered signal) is given by:

$$n = \left\lfloor \frac{\theta_{3dB} F_R}{6N} \right\rfloor . \tag{9.1}$$

Equation (9.1) is an important parameter that designers have to take into account when it comes to performance. The post-integration processing tries to take advantage of this multiple backscattered signals. There exists two ways to integrate the pulses. The distinction is made whether the pulses are sent from a coherent or a non-coherent transmitting source.

9.2 Principles

For the coherent integration process, a phase estimation is required in order to compensate for phase shifts between consecutive pulses. Then, the obtained signal-to-noise-ratio for n pulses is given by:

$$SNR_{ci} = SNR_{sp} + 10\log_{10}(n), \tag{9.2}$$

where SNR_{sp} denotes the signal-to-noise-ratio for a single pulse. For the non coherent integration process, the SNR is given by:

$$\begin{aligned} SNR_{nci} &= SNR_{ci} - 10\log_{10}(L_{nci}) \\ &= SNR_{sp} + 10\log_{10}(n) - 10\log_{10}(L_{nci}), \end{aligned} \tag{9.3}$$

where

$$L_{nci} = \frac{1 + SNR^{'}}{SNR^{'}}, \tag{9.4}$$

and

$$SNR^{'} = c + \sqrt{a + b}, \tag{9.5}$$

where

$$a = \frac{10^{\frac{SNR_{sp}}{10}}}{4n^2},$$

and

$$b = \frac{10^{\frac{SNR_{sp}}{10}}}{n},$$

and

$$c = \frac{10^{\frac{SNR_{sp}}{10}}}{2n}.$$

The following picture (figure 9.1) illustrates the NCI process for two different cases, aircraft and missile. We can see that the post-integration increases the overall SNR by almost $10dB$ which is quite interesting in such noisy environments. Coherent integration obviously provides better figures but at the unavoidable cost of more signal processing.

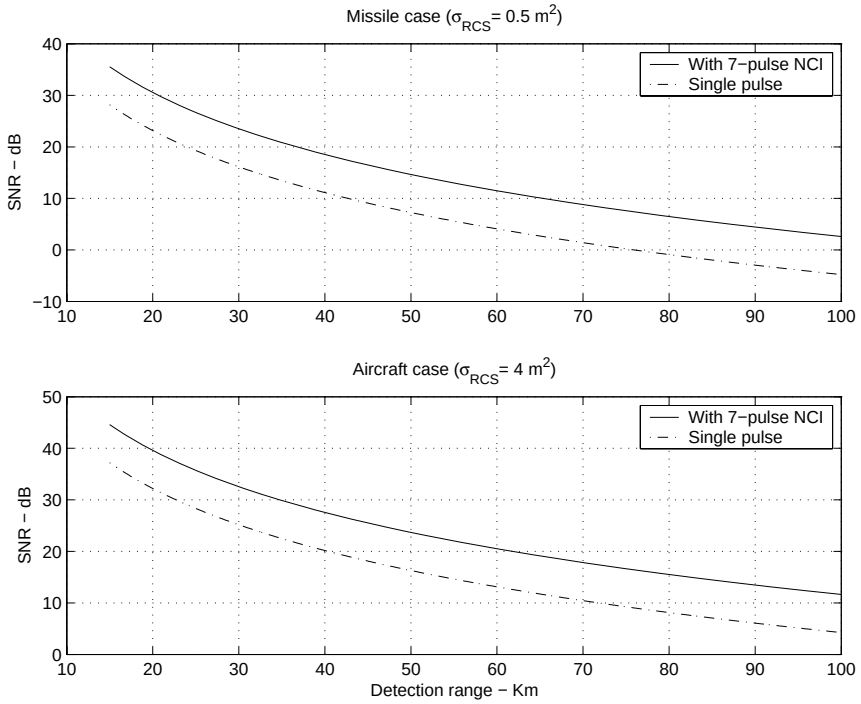

Figure 9.1: Post Integration example

Part III

Application Example

Chapter 10

Simulator and Models

10.1 Signal modeling

A Matlab© simulator has been developped at Thales Air Defence - TAD - facility in Bagneux (France), where I conducted this thesis. It has been decided to implement the simulator using Matlab© because radar signal processing techniques strongly consider matrices and filtering as support for data handling. Moreover, digital computation is faster implemented using Matlab© rather than C programming although C runs faster than Matlab©. The simulator is a block-based system where any algorithm can be run as a stand alone component. Moreover, the user can define a test scenario for the whole signal processing chain. The number of targets, their range and their velocity can be manually set. The use of a computer allows to have *almost infinite* memory storage. Thus, clutter maps are used to store up-to-date clutter information. A graphical tool allows the user to set the parameters of the scenario and it produces a parametric input file to the radar signal processing simulator.

10.2 Experiments and Plots

The following pictures illustrate the predefined scenario. Each picture depicts one step in the radar signal processing chain.

- Figure 10.1 represents the simulation parameters. In this scenario, there are two targets at different distances expressed in samples (cells) $d_1 = 200$ and $d_2 = 400$[1]. Each target has a different velocity expressed in terms of the repetition frequency F_R as $v_1 = 0.3 \times F_R$ and $v_2 = 0.7 \times F_R$.
  The figure shows the received echo is case of an ideal noise free environment. The transmitted signal is only affected by the natural attenuation due to the two ways trip[2].

[1]Note that in figure 10.1, targets appear to be at distance $d_1 = 400$ and $d_2 = 800$. This is due to an oversampling factor set to $N = 2$. Moreover, since the simulator has been developped in France, in the x-axis legend, the term "cases distance" refers to the cell notion defined in this thesis

[2]Sometimes called *attenuation profile*

- Figure 10.2 depicts the received signal at the input of the Pulse Compression stage. The signal looks like random white noise as explained earlier. In the simulator, complex AWGN with variance set to $\sigma^2_{noise} = 2dB$ is used. Note that each color defines a pulse within the pulse train.
- Figure 10.3 depicts the Pulse Compression box output : the output starts to show some important information. Two peaks emerge from the background noise ; i.e. two targets are detected[3]. Recall from equation (5.1) that the higher the compression rate, the higher the peak. However, it is obvious that hardware constraints prevent from having higher values for the compression rate.
- Figure 10.4 depicts the amplitude treatment box output : it modifies the received signal according to the algorithm. Thus, certain samples are replaced by a subsitute value in order to avoid false alarm increase.
- Figure 10.5 depitcs Doppler filtering operation : it discriminates targets according to their relative radial velocity. Here, the radar is assumed to have a fixed position. Note that if we had set one target to have a zero velocity, then it would have been filtered out since the figure is a snapshot at a given instant and it does not take into account wobulation advantage. A closer look into the figure show that each the target responds to two Doppler filters. This is due to the fact that the bank of Doppler filters is contructed such that it has overlapping frequency region in order to get fine accuracy in the frequency range considered. The module-logaritm calculation then reduces the dynamic range value.
- Figure 10.6 depicts the clutter estimate from the range CFAR algorithm. The algorihm is valid for the whole range. It appears that the first peak seems to be doubled. This is due to the fact that the algorithm works in a sliding way (c.f. equation (8.2) and (8.3)). Each cell can is used several times as long as it remains in the computation window.
- Figure 10.7 depicts the clutter esimate produced by the sea CFAR algorithm. It only shows the closer target at distance $d1 = 200$ cells in the 1D clutter map. This is due to the fact that the algorithm defines a maximum range at which the sea clutter power cannot be determine efficiently. This cut-off distance is set here to be $d_{cut} = 333$ cells. The *strange* look of the figure is due to the way cell clutter values are generated. Recall that for each cell set, a unique clutter power value is computed. Thus, in the range dimension, N_{range} cells will have the same clutter value, leading to a stairs-like figure.
- Figure 10.8 depitcs the clutter estimate produced by the ground CFAR algorithm. It shows both targets in the clutter 1D map. It looks like the output from the sea ACP but here the cut-off distance is set to $d_{cut} = 666$ cells.

Note that for both ACP outputs, targets position looks to have been shifted by a couple of cells in the radar direction. This is mainly due to Doppler shift that in time domain can be seen as a time delay ; i.e. a distance offset. Iterative processing using different carrier frequencies f_0, different repetition frequencies F_R tend to lower these consequences.
Finally, for each cell, a unique clutter map is designed where each cell have the value of the maximum of all three estimators. Then, an indicator of the presence of a target is set to true for each cell if and only if the clutter estimate[4] exceeds the selected threshold (c.f. equation (8.14)).

[3] At distance $d_1 = 200$ and $d_2 = 400$

[4] Clutter also contains usefull signal

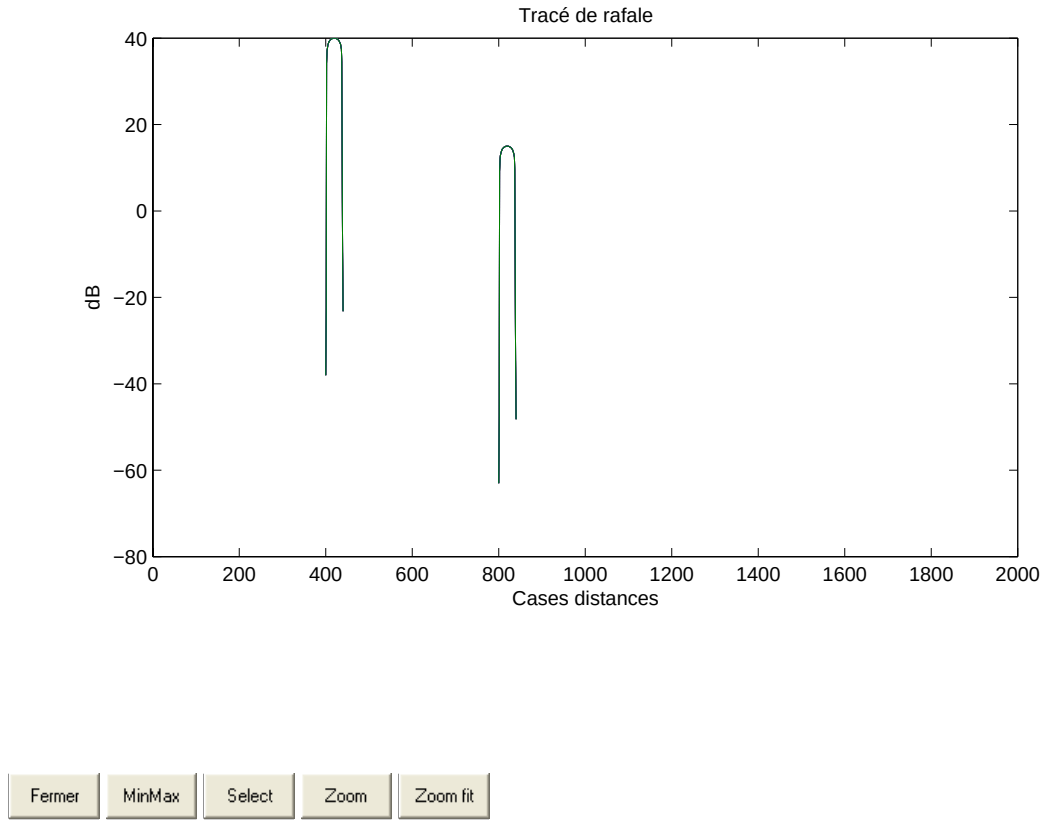

Figure 10.1: Noise Free targets echo

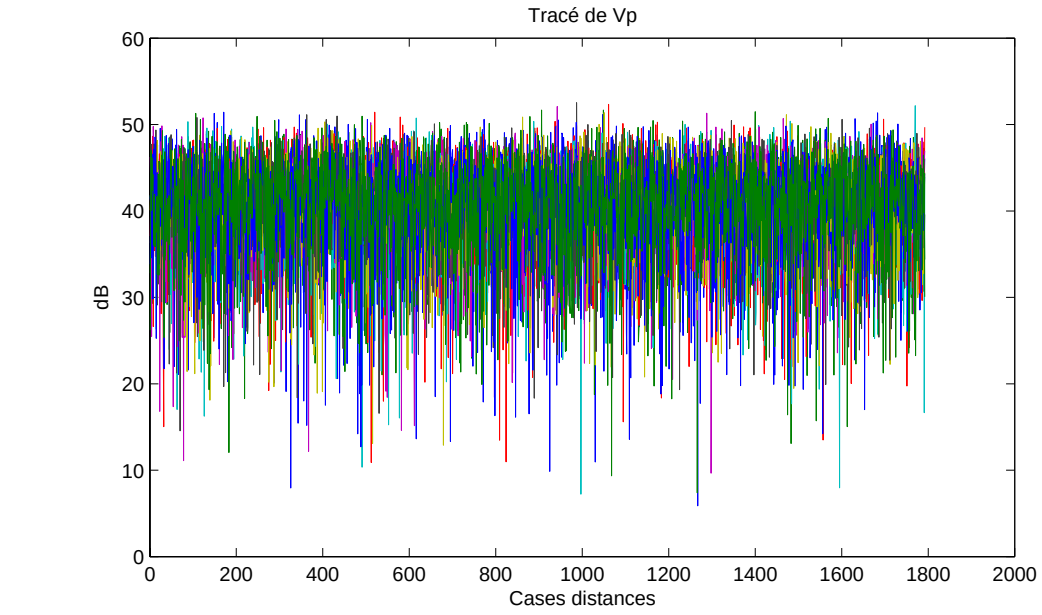

Figure 10.2: Received target echo

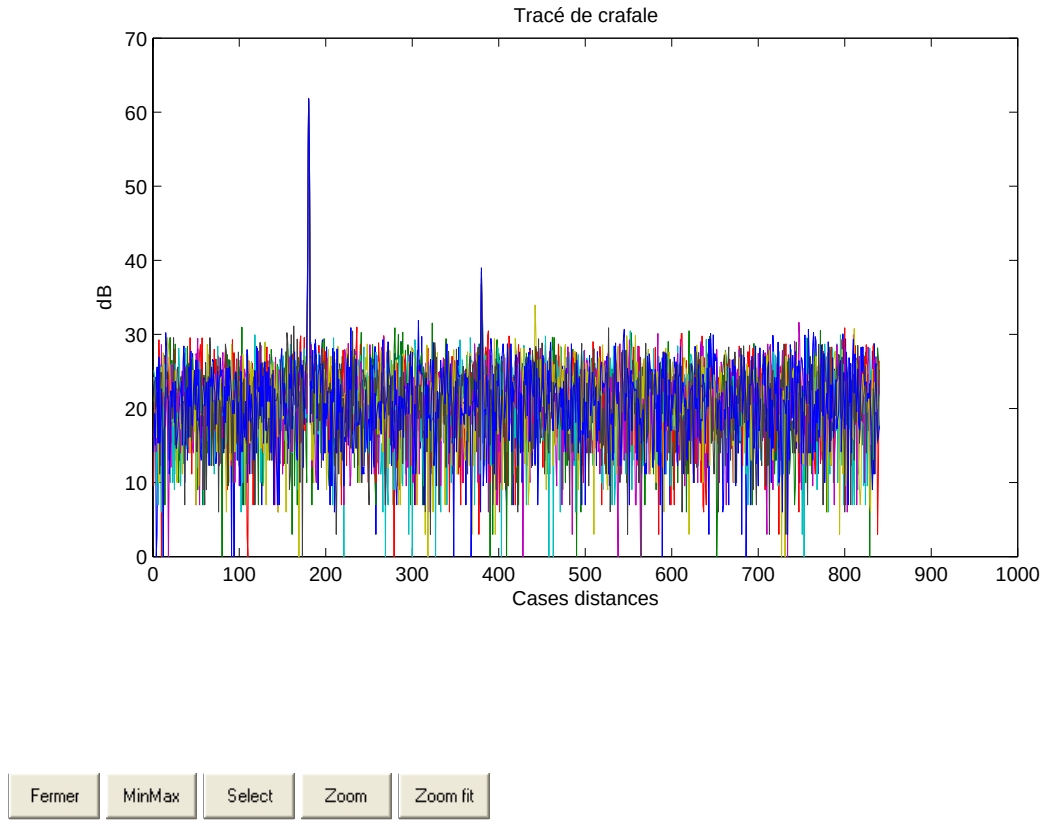

Figure 10.3: Pulse Compression output

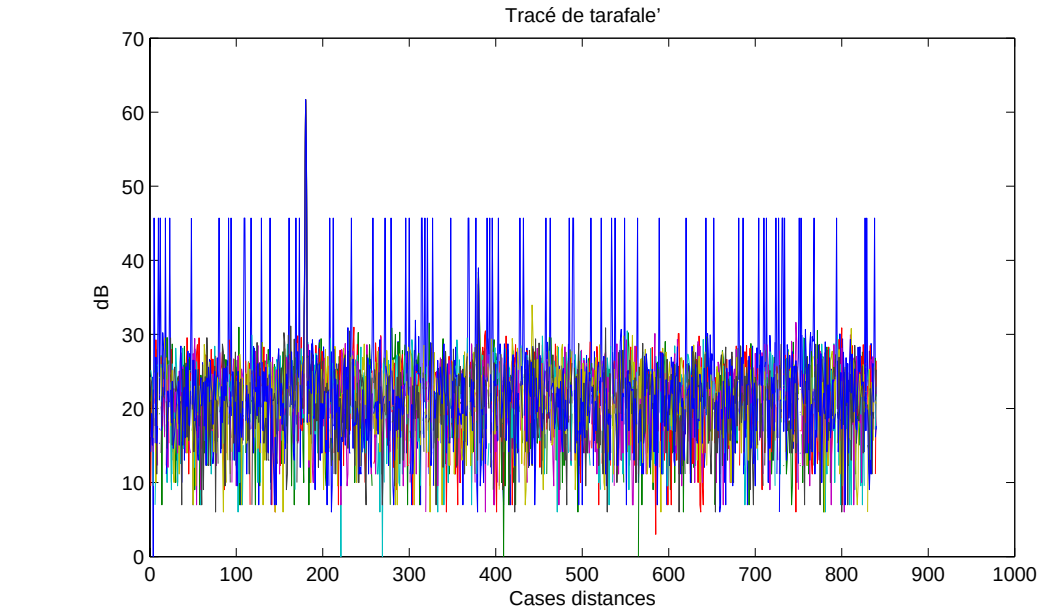

Figure 10.4: Amplitude Traitment output

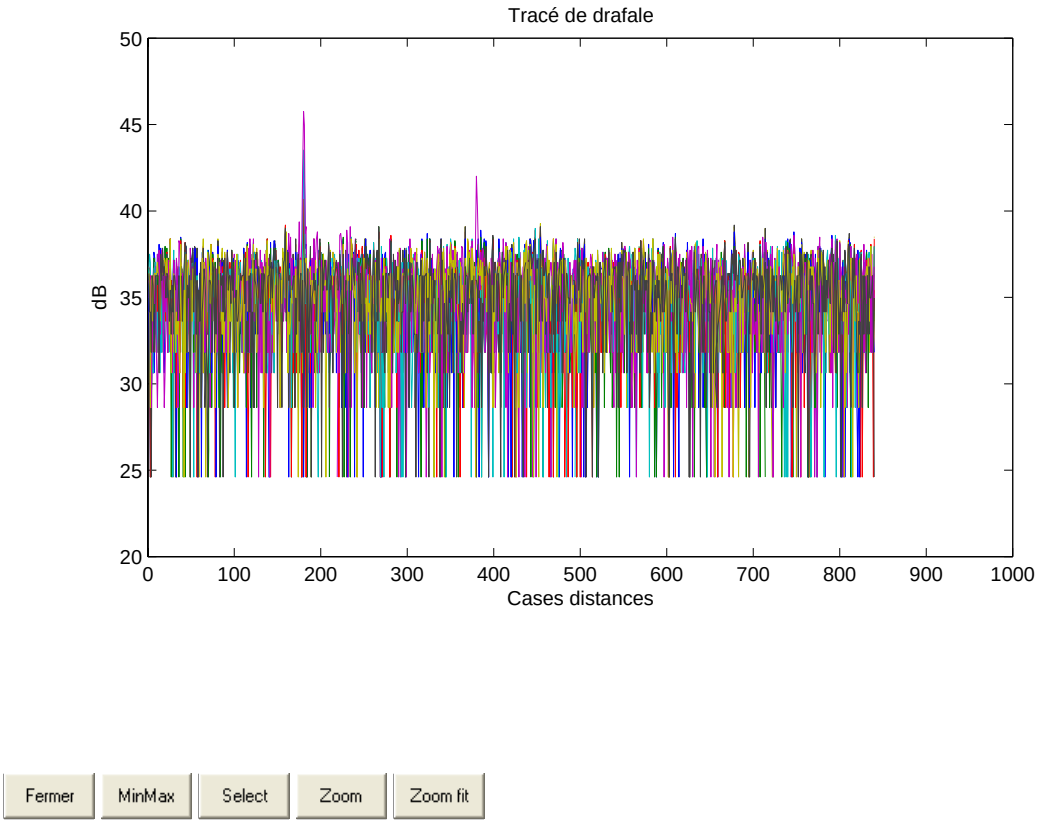

Figure 10.5: Doppler Filtering output

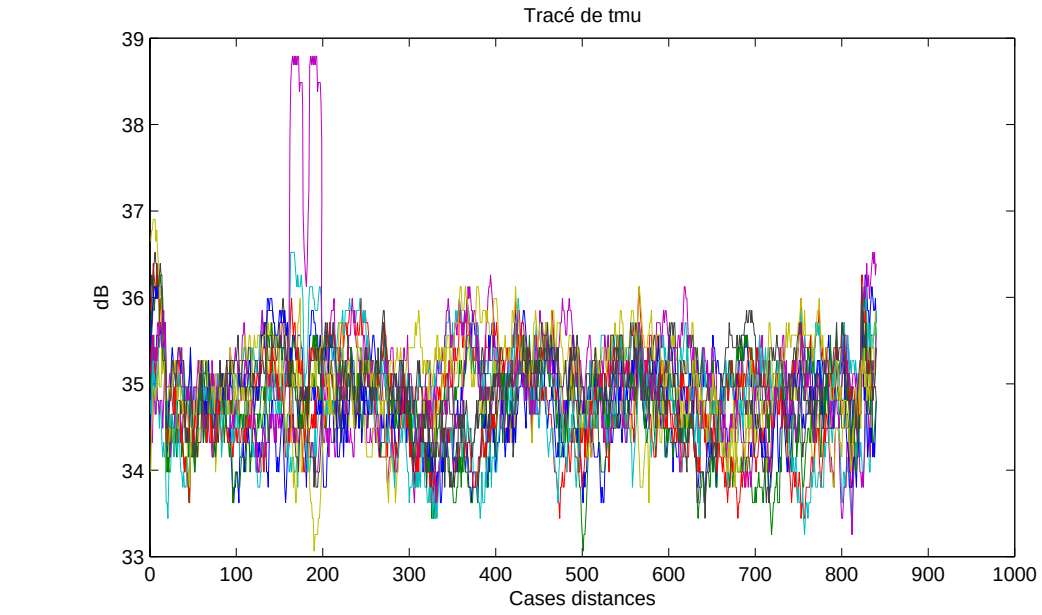

Figure 10.6: CFAR output

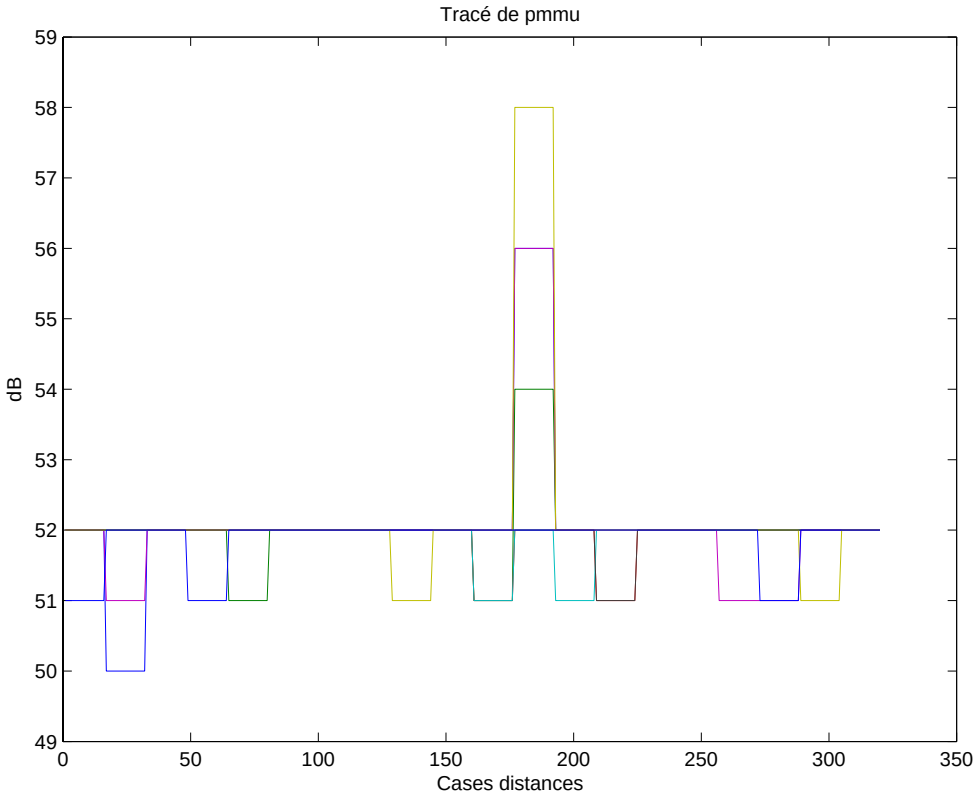

Figure 10.7: Sea ACP output

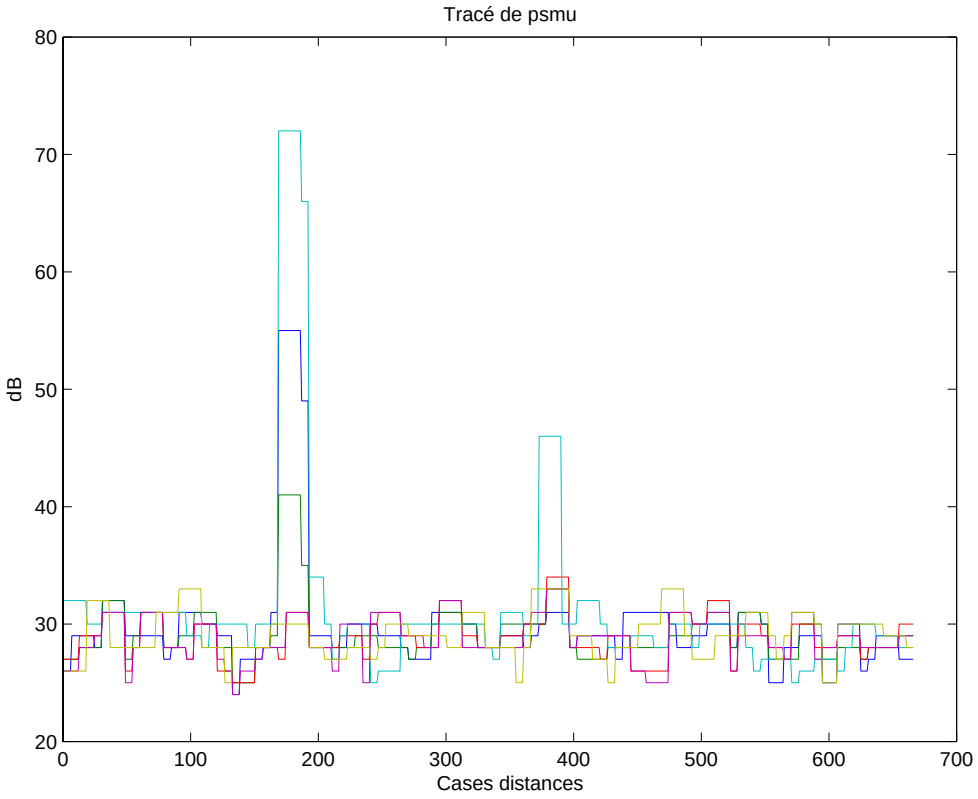

Figure 10.8: Ground ACP output

Conclusion

Radar systems have always been quite impressive from a performance point of view. Within the wide range of applications, radars are capable of detecting and/or tracking mobile targets, produce a weather map, evaluate vehicle speed. This wide range of applications leads to a variety of system architecure. However, from a global system overview, radars resemble each other. They all have signal generator, antenna (dual or not), mixer and filters. If we focus on signal processing involved in radar, it appears that techniques embedded in radars strongly differ according to the radar mission.
This thesis aims to present in details the signal processing techniques employed in a military radar. These techniques are strongly based on mathematics and specially on stochastic processes. Detecting a target in a noisy environment is a many folds sequential process. The signal processing chain only provides to the overall system boolean indicators stating the presence (or not) of targets inside the coverage area. It is part of the strategical operation of the radar.
The selection of signal procesing techniques according to the radar performance requirements is one of the most important step in military radar design. Signal processing, as we have seen throughout this paper, provides figures that tactical leaders take into account when looking for performances and capabilities. Nowadays, digital processing allows fast and efficient computation. The basic example is the use of FFT and IFFT to perform time-convolution (filtering).

My work at Thales Air Defence was twofold :

- I have ported old signal processing algorithms to run on Linux© machines. Then, I tried to make algorithms work more efficiently by using built-in Matlab© functions. I also enhanced the simulator from a user-interface point of view by adding a multi-scan mode. This mode is used for iterative algorithms such as ACPs. It allows to update clutter maps,

- I have provided a working document (this thesis) that best describes the MRR radar operation. The document mostly contents a balance between litterature ressources, theory knowledge and simulator outputs.

As a future work, one could focus on new antenna techniques that allow multiple beam to operate simultaneously. These new antennas provides supplementary ressources to track multiple targets. They are based on flat electronically steered arrays (SMBAA). Litterature on this topic allows the reader to make links between detecting a target and tracking it using such antennas and Kalman filtering theory.

Bibliography

[Ath03] F. Athley. *Space-Time Parameter Estimation in Radar Array Processing*. PhD thesis, Chalmers University of Technology, Department of Signals and Systems, Göteborg, Sweden, 2003.

[Bar75a] David K. Barton. Radars volume. In *Pulse Compression*, volume 3. Artech House, Inc., 1975.

[Bar75b] David K. Barton. Radars volume. In *Pulse Compression*, volume 7. Artech House, Inc., 1975.

[Car62] Michel-Henri Carpentier. *RADARS Théories Modernes*. DUNOD, 1962.

[Car87] Michel-Henri Carpentier. *Le RADAR*. Presses Universitaires de France, 1987.

[CCHF00] Liu Weixian Chang Chee Hang, Wong Char Ming and Jeffrey S Fu. Radar mti/mtd implementation and performances. *Second International Conference on Microwave and Millimeter Wave Technology Proceedings*, 2000.

[Col85] Henry W. Cole. *Understanding Radar*. COLLINS, 1985.

[D.O63] North D.O. An analysis of the factors which determine signal/noise discrimination in pulsed-carrier systems. *Reprinted in Proc. IEEE*, 51:1016–1027, July 1963.

[Hay96] Monson H. Hayes. *Statistical Digital Signal Processing and Modeling*. John Wiley & Sons, Inc., 1996.

[Joh97] Stephen S. Johnston. Target fluctuation models for radar system design and performance analysis : An overview of three papers. *IEEE Transactions on Aerospace and Electronic Systems*, 33(2), April 1997.

[LR52] Zadeh L.A. and J.R. Ragazzini. Optimum filters for the detection of signals in noise. *Proc. IRE*, 40:1223–1231, October 1952.

[MAK00] Mohammad Hasan Bastani Mohammad Ali Khalighi. Adaptive cfar processor for nonhomogeneous environments. *IEEE Transactions on Aerospace and Electronic Systems*, 36(3), July 2000.

[Sko80] Merrill I. Skolnik. *Introduction to Radar Systems*. McGraw-Hill Book Company, 2nd edition, 1980.

[Swe60] P. Swerling. Probability of detection for fluctuating targets. *Information Theory, IEEE Transactions*, 60:269–308, April 1960.

[Tho82] Léo Thourel. *Initiation aux techniques modernes des Radars*. CEPADUES Edition, 1982.

[Wat98] S. Watts. Cfar detection in spatially correlated sea clutter. *EUREL meeting on Radar and Sonar Signal Processing, Peebles*, July 1998.

[Win03] J. Wintenby. *Resource Allocation in Airborne Surveillance Radar*. PhD thesis, Chalmers University of Technology, Department of Signals and Systems, Göteborg, Sweden, 2003.